APPLICATION OF THE COMPONENT METHOD TO COLUMN BASES - EXPERIMENTATION AND DEVELOPMENT OF A MECHANICAL MODEL FOR CHARACTERIZATION

ir. S. Guisse, University of Liège
ir. D. Vandegans, CRIF-Steel Construction
Dr. J.-P. Jaspart, University of Liège

Research Centre of the
Belgian Metalworking Industry

MT 195 December 1996

Steel Construction Department

FOREWORD

In the mid-eighties, the MSM Department of the University of Liege initiated a long-term research work in the field of the beam-to-column joints. That resulted from a decision taken within the Task Working Group 8-1/2 of the European Convention for Constructional Steelworks to investigate the question of the actual structural response of the joints not only for what regards the joint properties properly, i.e. the strength, the stiffness and the ductility, but also the possible effects of such an actual response -in contrast with the usual assumption of either pinned or fully continuous joints- on the global analysis, i.e. the distribution of internal forces. According to what has for long become a common local stately, the Division of Steel Structures of CRIF, located in Liège, was associated to this important research task. If the contribution of CRIF was rather modest at the very beginning, it increased substantially during the last year due to the strengthening of the CRIF research staff.

Successively the Liège partners participated separately of most often jointly two ESCS research contracts as subcontractor(s) of ARBED Luxembourg, who was the direct beneficiary. Two research projects were also suggested and agreed upon in the frame of consecutive two years term research contracts CRIF-IRSIA. This fortunate combination of circumstances made the work carried out in Liège considered as one of the most substantial contributions in the field.

In such conditions the Belgian public authorities could do nothing else than join immediately the co-founders of the European COST action C1, the first to be accepted by the European Union in the field of Civil Engineering. The success of this international initiative is reflected by the tremendous increase of member countries and the need to organise this action in working groups and even in sub-task working groups. Because the European Union involvement in the COST actions does not consist in funding research but well meetings and seminars, it was up to the local authorities to provide the funds enabling a fruitful research that would feed this wide European initiative. The Government of the Walloon Region did not deceive the researchers' expectations and decided to allocate a significative research grant to the Liège teams in order to enable an in-deep theoretical, analytical, numerical and experimental study of the beam-to-column joints, beam splices and column bases.

The Liège partners had thus the opportunity to develop during more than 12 years, and that without interruption, a series of research works focused on quite connex items but the objectives of which were never duplicated but, on the contrary, developed in such a way to be harmoniously complementary.

A lot of publications in top-rank journals, contributions to colloquia and seminars, presentations upon invitation took place. A Ph.D thesis, an « habilitation »thesis, about a dozen of student 's terminal works are as many testimonies of the research activities developed in Liège.

There is no doubt that the beam-to-column joints and beam splices were among the first topics to be studied because of the need for a satisfactory answer to these items that indeed affect significantly the global

economy of the structural project. As a result the first draft of Annex J to Eurocode 3-Part 1: Steel Buildings was deeply revised and substantially implemented and it is while stressing that this tremendous and tedious work was conducted by a trio of young researchers whose one of the most active members is the senior author of present report. A similar work is being completed by the same trio (with some additional assistance received from the COST C1 Working Group on "Steel and Composite Connections" ant the Technical Committee 11 "Composite Construction" of the European Convention of the Constructional Steelwork") for composite beam-to-column joints and beam splices.

The deep synergy that is existing between the MSM Department, whose objectives first -though not only- focus on basic research and the Division of Steel Structures, whose aims is especially to fulfil the needs of the profession, is testified in one of the best manners by the issue of quite valuable design aids. First the so-called SPRINT document (*) - because it has been developed in the frame of the European SPRINT action - was produced in 1994; the general procedure described in Annex J of Eurocode 3 - Part 1 may there be used straightforward due to safe simplifications that are still in compliance with the design principles of Eurocode 3. There calculations procedures can be applied in by-hand calculations. Second, design tables were established for a large though limited number of standard joints; they give directly, for a given joint between given column and beam (or beam and beam) all the strength and stiffness properties of the joint as well as indications on the joint component that governs strength and the class of this joint.

At the time the present report will be published , an additional quite valuable document will be available: the so-called « Manual on Frame Design Including Joint Behaviour ». This manual (**) prepared under the auspices of the European Convention for Steel and Coal -in short ECSC- not only covers the background dealing with the joint behaviour and characterisation but also all the interferences between the joint structural response and the global frame analysis and the design checks. This manual contains first the elementary theoretical background enabling to grasp the several items, then the applications rules that are relevant to the latter, last fully documented worked examples. This manual has a companion: a floppy diskette that may assist the designer in his task of conceiving and designing beam-to-column joints or beam splices according to the SPRINT method or to the most sophisticated design procedure of Annex J of Eurocode 3 - Part 1. This software is undoubtfully aimed at becoming the designer's companion in any circumstance where joints are of concern.

It remains that the special type of joint which is the one where a column is connected to its foundation, the latter lying for its own on the ground was still to be investigated. This question is not less of concern than beam-to-column joints for what regards their effects on global analysis, despite the fact they are usually much less. The fact is that the knowledge in the field of column bases is much less and that, in addition, column base behaviour involves some consideration of soil mechanics. A substantial improvement in the field implies especially a lot of experiments and requires to differentiate between the column-to-concrete connection and the concrete-to-soil connection. In accordance with a now well accepted concept, the one of the component method which has successfully demonstrated its capabilities when investigating the aforementioned types of joints, the analysis of column bases shall follow a similar approach. Present report comments on the experimental investigations conducted on the column-to-concrete connection components. Chronologically a first series of relevant tests were conducted in the frame of the COST action funded by the Walloon Region and a statistical evaluation of these tests had been performed two years ago. The evolution of the basic ideas substantiating the present design philosophy regarding joints made that

additional tests were conducted quite recently in order to assess the influence of additional parameters and to implement the previous evaluation of test results; this extent of the research work was conducted mainly by the junior author of the present report with the guidance and assistance of the senior one. The out xxx of this work is still in discussion and is therefore not included in the present report.

As it is now the report is still a research report, though it contains yet quite interesting information for design purposes. It is expected that in the near future, but provided some funds be devoted accordingly, the problem of column bases could provides answers of the same nature as those available for beam-to-column joints, i.e. very practice-oriented ones.

The responsibles of the department MSM and of the Division of Steel Structures of CRIF are both pleased to introduce this research report which undoubtfully will constitute a reference document for all those who are interested in the design and behaviour of column bases.

R.MAQUOI
Professor
Department MSM

E.PIRAPREZ
Division Manager
CRIF

(*) SPRINT Contract RA351 : Steel moment connections according to Eurocode 3 : Simple design aids for rigid and semi-rigid joint. Partners : CRIF (Liège, B); MSM Université de Liège (Liège, B); CTICM (Saint Rémy-lès-Chevreuse, F); ENSAIS (Strasbourg, F); Universita degli studi di Trento (Trento, I); LABEIN (Bilbao, E).

(**) Manual on frame design including joint behaviour : ECSC Contract n° 7210-SA/212 and 7210-SA/320. Partners : MSM Université de Liège (Liège, B); CRIF (Liège, B); RWTH (Aachen, D); TNO (Delft, NL); CTICM (Saint Rémy-lès-Chevreuse, F).

ABSTRACT

Column bases transfer reactions from the structure to the foundation.
When subjected to normal forces, shear forces and in-plane bending moments, they deform, particularly in rotation. This rotational behaviour is usually idealized as pinned or fully rigid. But in most of the cases, column bases have a so-called intermediate semi-rigid behaviour which influences significantly the global frame response.

In this report, laboratory tests recently performed in Liège on column bases with base plates including two or four anchor bolts are described and their main behavioural features are discussed. A simple analytical model for resistance evaluation is presented. Lastly a refined mechanical model able to predict the whole response of the column bases from the first loading steps to failure is described.

These two models are based on the component method which has been implemented in the revised Annex J of Eurocode 3 [3]. According to the component method, any structural joint is considered as a set of individual components and the determination of its mechanical properties as strength and rotational stiffness includes three main steps :(i) definition of the constitutive components, (ii) evaluation of their mechanical properties and (iii) assembly of the components so as to derive the properties of the whole joint.

To extend this concept to column bases, Eurocode 3 rules for components have been amended and original procedures for assembly have been developed and included in the above-mentioned models.
Lastly, comparisons of the two models with the experimental tests are performed and conclusions on the suitability of the followed approaches are drawn.

RESUME

Les pieds de colonnes transmettent les réactions de la structure à la fondation. Lorsqu'ils sont soumis à un effort normal, à un effort de cisaillement, ou encore à un moment de flexion dans le plan, ils subissent des déformations et particulièrement une rotation. Leur comportement vis-à-vis de cette rotation est habituellement idéalisé par une rotule parfaite ou par un encastrement tout à fait rigide. En réalité, dans la plupart des cas, les pieds de colonnes ont un comportement intermédiaire à celui de ces deux cas extrêmes; il s'agit d'un comportement appelé semi-rigide qui influence de manière significative les sollicitations de la structure globale.

Des essais en laboratoire ont été effectués récemment à Liège sur des éléments de colonnes avec des plaques de base fixées à la fondation à l'aide de deux ou de quatre boulons d'ancrage. Les résultats de ces essais sont décrits dans le présent rapport où sont également commentées les influences des différents facteurs qui déterminent le comportement d'un tel assemblage. Un modèle analytique relativement simple, permettant de déterminer la résistance de la connexion, est présenté. En dernier lieu, un modèle mécanique capable de prévoir le comportement complet des pieds de colonnes depuis le début de l'application des charges jusqu'à la rupture, est présenté.

Ces deux modèles de calcul sont basés sur la méthode des composantes qui a été introduite dans la nouvelle version de l'Annexe J de l'Eurocode 3 [3]. En application de cette méthode, toute connexion

dans une structure est considérée comme un ensemble de composantes individuelles et la détermination des caractéristiques mécaniques de tout l'assemblage, aussi bien sa résistance que sa rigidité en rotation, s'effectue en 3 étapes : (i) définition des composantes, (ii) évaluation des caractéristiques mécaniques de chacune d'entre elles et (iii) assemblage du comportement de chacune des composantes de manière à en déduire les propriétés de la connexion tout entière.

Afin d'étendre ce concept au cas des pieds de colonnes, les lois de comportement des composantes données dans l'Eurocode 3 ont été adaptées, et des procédures originales pour leur assemblage ont été développées; elles sont introduites dans les modèles précités.
Enfin, les résultats des essais sont comparés aux résultats obtenus par les modèles de dimensionnement et la fiabilité de ceux-ci est évaluée.

SAMENVATTING

De kolomvoetverbindingen brengen de reactiekrachten van de structuur over op de fundering. Indien de kolomvoet onderworpen is aan een normaalkracht, een afschuivingskracht of een buigingsmoment in het vlak zal hij een vervorming ondergaan en dan specifiek een rotatie. Dit gedrag wordt meestal voorgesteld als een perfecte scharnier of als een inklemming. In werkelijkheid hebben kolomvoeten een gedrag dat tussen deze twee uitersten is te situeren. Het gaat hier om een zogenaamd semistijf gedrag dat de krachtenverdeling in de structuur ernstig veranderd.

Onlangs zijn er in Luik laboratoriumproeven uitgevoerd op kolomvoeten die met twee of vier ankerbouten aan de fundering verbonden waren. De resultaten van deze proeven zijn in dit rapport weergeven alsook de commentaren over de verschillende factoren die het gedrag van zulk een verbinding beïnvloeden. Er wordt een vrij eenvoudig analytisch model om de weerstand van een verbindingte bepalen voorgesteld. Tenslotte wordt er een mechanisch model voorgesteld dat in staat is het volledige gedrag van de kolomvoet te voorspellen. Dit model werkt vanaf de eerste beklastingsstappen tot het bezwijken van de kolomvoet.

Beide modellen zijn gebaseerd op de methode van de samengestelden die werd ingevoerd in de nieuwe versie van bijlage J van Eurocode 3 [3]. Volgens deze methode is elke verbinding op te splitsen in individuele componenten. De bepaling van de mechanische eigenschappen, zowel weerstand als stijfheid gebeurt in drie stappen: (i) bepaling van de componenten, (ii) bepaling van de mechanische eigenschappen van elke component en (iii) samenstellen van de componenten zodat de eigenschappen van de volledige verbinding duidelijk worden.

Teneinde dit concept te kunnen uitbreiden naar het geval van kolomvoeten, werden de in Eurocode 3 gegeven formules, voor het gedrag van de componenten, aangepast. Er werden nieuwe procedures opgesteld om het samenstellen van de componenten te regelen; zij zijn in de hiervoor vermelde modellen verwerkt.

Tenslotte, zijn de testresultaten vergeleken met de resultaten van de berekeningsmodellen en werd de betrouwbaarheid van deze laatste gecontroleerd.

CONTENTS

1. INTRODUCTION

Column bases constitute the link between frame and foundation and so represent quite important structural elements. Those considered in this report are constituted of concrete blocks embedded in the foundation on which the column steel profile is connected by means of a base plate welded at the column end and maintained on the concrete block by two or four anchor bolts.

When subjected to normal and shear forces and to in-plane bending moments, these column bases deform, particularly in rotation. This rotational behaviour is usually idealized as pinned or fully rigid. But in most of the cases, column bases exhibit an intermediate behaviour, termed semi-rigid, as well as a limited resistance to applied forces. The semi-rigid behaviour of column bases influences the structural response of the whole frame and in particular the lateral deflections and the global frame stability in sway frames, the column stability in non-sway frames. Take this semi-rigid effect into account in the frame analysis and design process is known to lead to significant cost savings linked to the reduction of the manpower necessary to realize rigid column bases (less stiffening) or to the reduction of the column and/or beam size in the case of pinned column bases.
This required however to define the design properties of the column bases in terms of stiffness and resistance. The present report is aimed at presenting recent developments in this field.

In a column base, two rotational deformabilities need to be distinguished :

- the deformability of the connection between the column and the concrete base foundation *(column-to-concrete connection);*
- the deformability of the connection between the concrete base and the soil *(concrete-to-soil connection)*

For a typical column-to-concrete connection, the bending behaviour is represented by a M-ϕ curve, the shape of which is influenced by the ratio of the bending moment to the axial load at the bottom of the column.

For the connection between the concrete foundation and the soil, two basic deformability curves are identified:

- a N-u curve which corresponds to the soil settlement due to the axial compressive force in the column; in contrast with the other types of joint, this deformability curve may have a significant effect on the frame behaviour;
- a M-ϕ curve characterizing the rotation of the concrete block in the soil.

The deformability of the column base due to the shear force in the column may be neglected.

The column-to-concrete and concrete-to-soil connection M-ϕ curves are combined in order to derive the rotational stiffness at the bottom of the column and conduct the frame analysis and design accordingly.

Similar deformability sources exist in column bases subjected to biaxial bending and axial force. The connection M-ϕ curves are then defined respectively for both the major and minor axes.

In this report, only the rotational behaviour of the column-to-concrete major axis connections under uniaxial bending is investigated. The study of the concrete-to-soil connection requires the collaboration of experts in structures and geotechnics and is now the object of researchers performed in the frame of the new European Project COST C6.

The present reports reflects the common activities of the Department MSM of the University of Liège and the Steel Department of CRIF during these last years in the field of column bases; it includes three main parts :

- The results of 12 experimental tests on column bases with two and four anchor bolts and the discussion of their main behavioural features.
- The proposal of a simple analytical model for resistance evaluation.
- The development of a rather sophisticated mechanical model allowing to follow step by step the loading of the column base until collapse is reached through a detailed study of the evolution of the displacements and stresses in the different components of the column base.

The validity of the proposed models is then shown through comparisons with the experimental results.

Both models refer to the so-called component method. This concept has been recently included in Eurocode 3 and 4, and more particularly in their annexes J devoted respectively to the design of steel and composite beam-to-column joints and beam splices in building frames.

According to the component method, any joint has to be considered no more as a whole but as a set of basic components. Each of these basic components possesses its own strength and stiffness either in tension, in compression or in shear. The coexistence of several load components within the same joint element can obviously lead to stress interactions that are likely to decrease both strength and stiffness of the individual basic components.

The application of the component method requires the following steps:

a) *identification* of the activated components in the joint been considered;

b) *evaluation of the stiffness and/or strength characteristics* for each individual basic component (specific characteristics - initial stiffness, design strength, - or whole deformability curve);

c) *assembly* of all the components involved in the joint and evaluation of the stiffness and/or strength characteristics of the whole joint (specific characteristics - initial stiffness, design resistance, ... - or whole deformability curve).

The assembly procedure consists in deriving the mechanical properties of the whole joint from those of all the individual constitutive components. That requires a preliminary distribution of the forces acting on the joint into internal forces acting on the components in a way that satisfies equilibrium and respects the behaviour of the components.

In Annex J of Eurocodes 3 and 4, the analytical assembly procedures are described for the evaluation of the initial stiffness and the design moment resistance of the joint; these two properties enable to build design joint moment-rotation characteristic whatever the type of analysis.

The application of the component method requires a sufficient knowledge of the behaviour of the basic components. The combination of the components included in Eurocode 3 and Eurocode 4 allows one to cover a wide range of joint configurations, what should be largely sufficient to satisfy the needs of practitioners as far as beam-to-column joints and beam splices in bending are concerned.
For column bases, specific components are activated as "anchor bolts in tension" or "concrete in compression" and the loading is different from that presently covered by Eurocodes 3 and 4 as high axial forces are to be transferred to the foundation in addition to bending moments and shear forces.

These aspects are discussed in the report and original solutions are proposed.

Before ending this introduction, the authors would like to draw the attention of the reader on the difficulty to compare models and test results in an appropriate way. In order to avoid any misunderstanding and so as to demonstrate the grounds of the comparisons as they are performed in the present report, it is warmly recommended to the reader to have first a detailed look on the Annex to the present report before starting to study the document in itself.

2. EXPERIMENTAL TESTS

2.1 Test set-up and general configuration of the specimens

Twelve experimental tests on column bases have been recently carried out in Liège. The general configuration shown in Figure 2.1 is identical for all the tests. For technical reasons the tests were carried out with a compressive force F_1 in the column acting horizontally whereas the force F_2 generating bending moment was acting vertically.

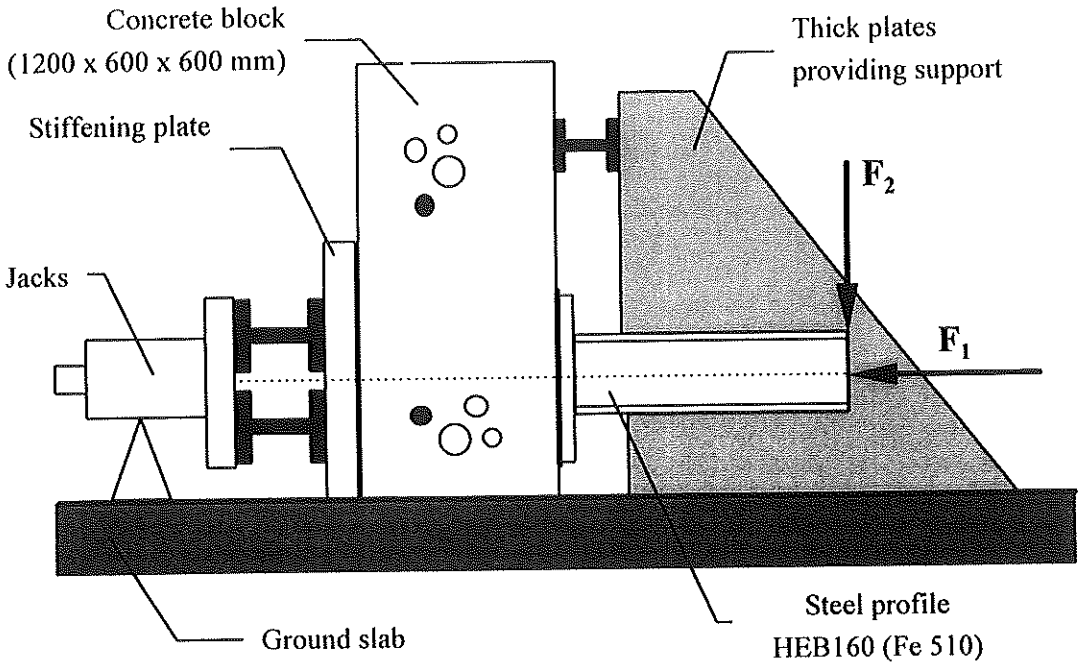

Figure 2.1- Test set-up.

The compressive force F_1 is applied by means of two jacks acting on the rear face of the concrete block. Thanks to the extremely thick stiffening plate (10 centimetres), the distribution of the stresses inside the concrete block may be considered to be the same as it would be if the block was placed directly on the ground.

Similar concrete blocks are used for all the tests : 1200 mm high for a 600 x 600 mm square base. All the blocks were concreted at the same time in order to ensure that their mechanical behaviour is as homogeneous as possible.

To prevent any movement of the block, a efficient support against the moment created by force F_2 was formed by two large thick steel plates placed on each side of the column profile (see Figure 2.1). In order to be able to resist applied stresses, the concrete block has been slightly reinforced. The reinforcements, however, are placed so as not to prevent the possible formation of cracks under the action of the compressive force, as it could happen in practical situations.

A thin layer of grout has been placed between the base-plate and the concrete block so as to ensure a good contact. Two types of test configurations were envisaged, with four (Figure 2.2) or two (Figure

2.3) anchor bolts. In the first case, the column base is nearly rigid, while in the second it is usually considered as pinned.

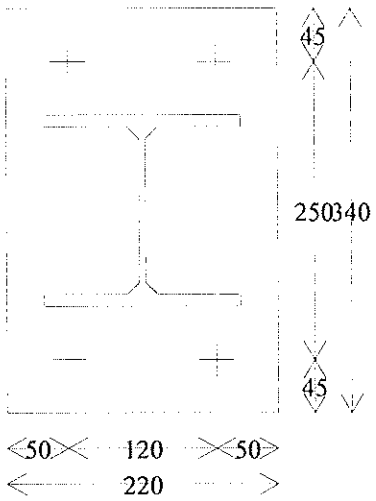

Figure 2.2- Plate with four anchor bolts.

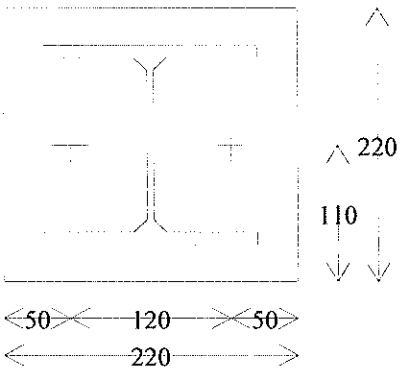

Figure 2.3 - Plate with two anchor bolts.

Only one steel column profile was considered in the test serie : HE160B. Its steel grade is S355.
The base-plates are welded to the column; the throat radius is 6 mm. Two different thicknesses are used for base-plates: 15 mm and 30 mm. The steel grade is also S235.
Anchor bolts M20 10.9 are used. They are made from steel rods curved as shown in Figure 2.4

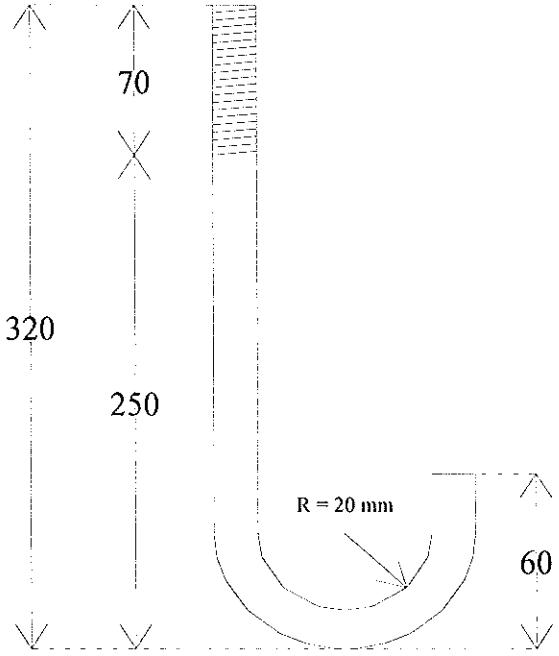

Figure 2.4 - Anchor bolts.

The same loading history is applied to all the tests (Figure 2.5) : preliminary application of the full compressive force on the column (F_1), which remains then constant, followed by a progressive application of the force F_2 until collapse.

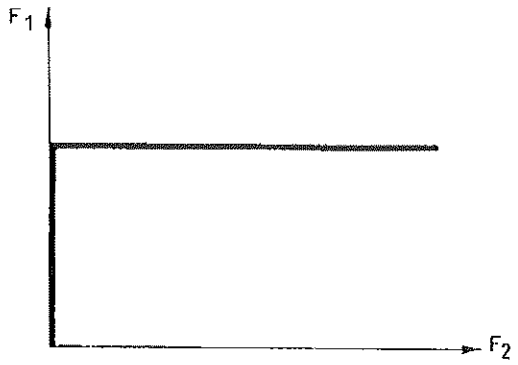

Figure 2.5 - Loading history

Table 2.1 gives the nomenclature of the tests and the value of the parameters which differentiate the test specimens. The designations given to the tests consist of the initial letters "PC", followed by three numbers: the first indicates the number of anchor bolts (2 or 4), the second relates to the thickness of the plate (15 mm or 30 mm) while the last gives the value of the axial load applied to the column, in kN. The initials PC mean « Pied de Colonne », what means nothing else than « column bases » in French.

Name	Anchor Bolts -	Plate thickness mm	Normal force kN
PC2.15.100	2	15	100
PC2.15.600	2	15	600
PC2.15.1000	2	15	1000
PC2.30.100	2	30	100
PC2.30.600	2	30	600
PC2.30.1000	2	30	1000
PC4.15.100	4	15	100
PC4.15.400	4	15	400
PC4.15.1000	4	15	1000
PC4.30.100	4	30	100
PC4.30.400	4	30	400
PC4.30.1000	4	30	1000

Table 2.1 - Nomenclature of the tests.

All of the data relative to the dimensions, geometrical and mechanical characteristics of the different components of the test specimens are outlined in the following section.

2.2 Measured geometrical and mechanical characteristics

One of the main components in column bases is, of course, the concrete. To determine its mechanical properties, six tests on cubes were cast at the same time than the foundation blocks. They were also tested few days after the column bases, i.e. about two months after the concreting.
The results of the compression tests on the cubes are given in Table 2.2. All the cubes were 158 x 158 x 158 mm ones (cross-section of 24964 mm²). The very low scatter of the results and the quite high impressive quality of the concrete are to be noted.

Cube No.	Ultimate load *kN*	Strength *MPa*	Young's Modulus *MPa*
1	1135	44.6	34200
2	1150	45.19	35100
3	1185	46.57	36700
4	1120	44.01	33600
5	1150	45.19	34500
6	1175	46.17	35900
Mean value		**45.29**	**35000**

Table 2.2 - Actual mechanical characteristics of the concrete.

The nominal dimensions of the steel bases-plates are shown in Figure 2.2 and Figure 2.3. For what regards their strength, tensile tests carried out in the laboratory revealed that their yield stress amounts 280 MPa while their ultimate strength is about 412 MPa, both for the 15 mm and the 30 mm plates.

The dimensions of the steel profile were measured on different specimens. As it has been asked to the manufacturer, all the beams were from the same rolling pass, so exhibiting a very low scatter for what regards geometrical and mechanical properties. For each test, the following values were therefore adopted as mean actual dimensions:

- total depth of the section ..... 164.7 mm
- width of the flanges .... 160.35 mm
- web thickness ..... 8.3 mm
- thickness of the flanges ..... 13.35 mm

- fillet radius..... 15 mm

The mechanical characteristics were also measured in laboratory:

- yield stress .....464 MPa
- ultimate stress.....580 MPa

High-strength steel was used for column profiles so as to prevent yielding of the column cross-section as far as possible and so as to concentrate the deformability and the failure mode in the column base. This was achieved, except in the last test, PC4.30.1000, where high stresses were obtained in the column.

From the measured characteristics of the steel profile, the following geometrical quantities, which will be useful in the remainder of this report, can be derived :

- Moment of inertia (major axis) ..... 2801.9 cm^4
- Area .....56.2 cm^2
- Reduced area (shear force).....11.4 cm^2

The anchor bolts exhibit a quite special behaviour. In fact, although their base metal is of very good quality (ultimate strength of about 1000 MPa but with good ductility), various phenomena tend to reduce the strength which can be expected:

- the shaping, carried out in the laboratory, consisted in bending a rod at 180 degrees (see Figure 2.4). To prevent microcracks from occurring in the curved zone, the metal was heated considerably, thereby reducing the strength of the material.
- in the concrete, the anchor bolts are fixed to bars embedded in the block. Unfortunately, for some tests, an initial unbending of the curved rod was observed before the ultimate resistance of the rod in tension is reached.

Consequently, even if a tensile test on a straight anchor bolt yields a strength of 250 kN, specific tests carried out on bolts fixed in the concrete block revealed a lower strength, i.e. 187 kN.

2.3 Instrumentation.

Three types of measurement devices were used:

- the displacement transducers D_1 to D_7;
- the rotational transducers ROT_1 and ROT_2 (direct measurement of the absolute rotations);
- the bolt strain gauges, placed in the anchor bolts, J_1 and J_2.

Figure 2.6 and Figure 2.7 show the positions of the various transducers used for the tests with four anchor bolts. A similar arrangement is used for configurations with two anchor bolts. The only difference is the position of the D_2 and D_4 transducers, which are located closer to the column flanges.

Transducers D_6 and D_7 are just there to detect any overall rotation of the concrete block under the action of force F_2. In fact, the supports used were so rigid that this movement proved to be completely negligible.

Transducers D_2 to D_5 give a rather good picture on how the base-plate deforms relatively to the concrete block. Transducer D_1 is the most important one as it measures the transverse displacement of the steel column in the direction of the force F_2.

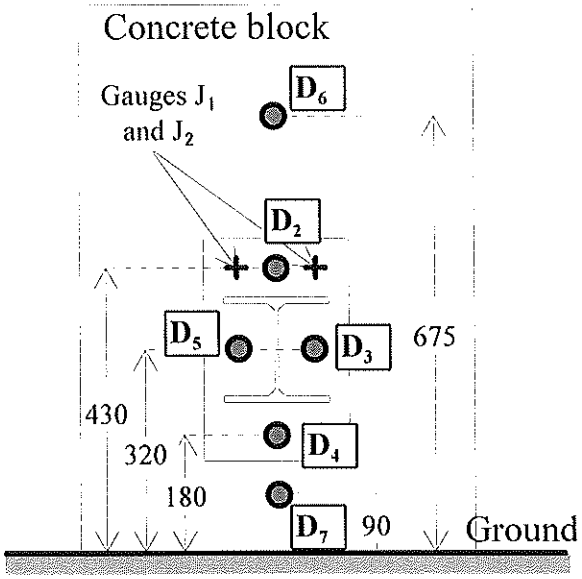

Figure 2.6 - Instrumentation (front view)

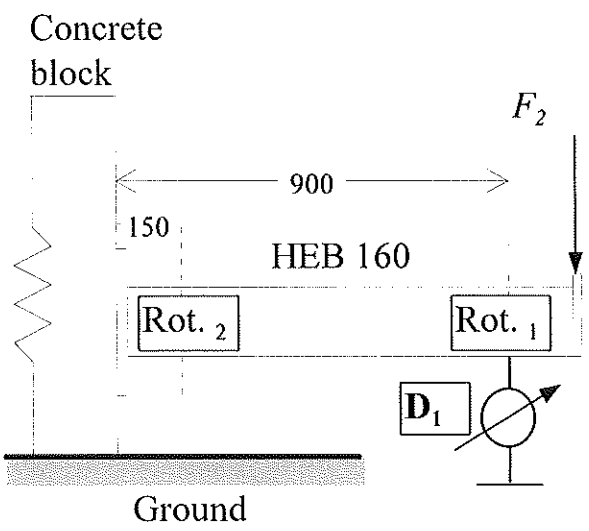

Figure 2.7 - Instrumentation (side view).

Rotational transducers ROT_1 and ROT_2 (Figure 2.7) give a direct measurement of absolute rotations along the column. These instruments are of great accuracy. They represent an excellent mean to obtain reliable moment-rotation curves.

Finally, cylindrical gauges J_1 and J_2 are glued in a hole drilled in the centre of the two anchor bolts where tension is likely to occur. They measure the strain at the centre of the shank of the bolt, at a place where the stresses can be considered as uniform. In practice, the top of the gauge was placed at least two centimetres beneath the bottom face of the nut.

2.4 Moment-Rotation Curves

2.4.1 Derivation of the curves.

2.4.1.1 Introduction.

Through the measurements outlined in the previous paragraphs, the moment-rotation curve of the column bases may be derived. How to combined rough measurements carried out during the tests to get moment and rotation at each loading step requires few explanations. This is the subject of the following paragraphs.

2.4.1.2 Expression of the bending moment in the column base.

Because of the considerable amount of deformability and the high magnitude of the normal forces in the column, second order effects cannot be ignored. In fact, Figure 2.8 shows that the bending moment in the column base, although mainly due to the force F_2, is influenced by the compressive force F_1 in the column. The latter acts along a direction represented by the dotted line in Figure 2.8; this direction changes during the test. It may therefore be resolved into two components: a horizontal and a vertical one. The first one creates an additional moment due to its eccentricity (measured at the level of the base-plate). The second component acts along the same direction than F_2 but tends to reduce the bending moment.

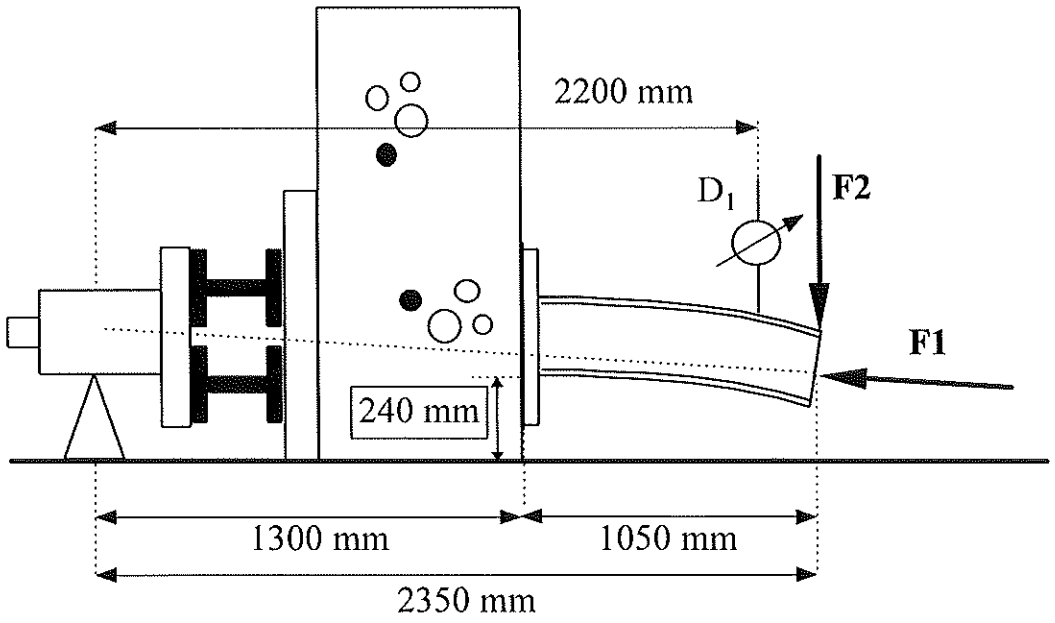

Figure 2.8 - Determination of the bending moment in the column base.

The action line of the force F_1 has an inclination termed α.The α value is:

$$\alpha \approx tg\alpha = \frac{D_1 \text{ (en m)}}{2{,}2} \tag{2.1}$$

The moment on the column base writes:

$$M = (F_2 - F_1.\sin\alpha).1{,}05 + F_1.\cos\alpha.(tg\alpha.1{,}3) \tag{2.2}$$

In equation (2.2), F_1 and F_2 are expressed in meters, while the bending moment is in kNm. By replacing α by its expression (2.1) and by considering that the angle α is rather small, the following definition of M is obtained :

$$\begin{aligned} M &= (F_2 - F_1.\sin\frac{D_1}{2,2}).1,05 + F_1.\cos\frac{D_1}{2,2}.(D_1.\frac{1,3}{2,2}) \\ &= (F_2 - F_1.\frac{D_1}{2,2}).1,05 + F_1.(\approx 1).D_1.0,591 \\ &= 1,05.F_2 + 0,114.F_1.D_1 \end{aligned} \qquad (2.3)$$

In this expression, the first term relates to the first order, whereas the second term represents the additional moment produced by the second order effects. D, F and M quantities in equation (2.3) are expressed respectively in m, kN and kNm.

Figure 2.9 shows the comparison between the first and second order curves M-D_1 for the test where the difference is the largest - test PC2.30.1000. For the tests with a small compression load, the difference is usually rather limited.

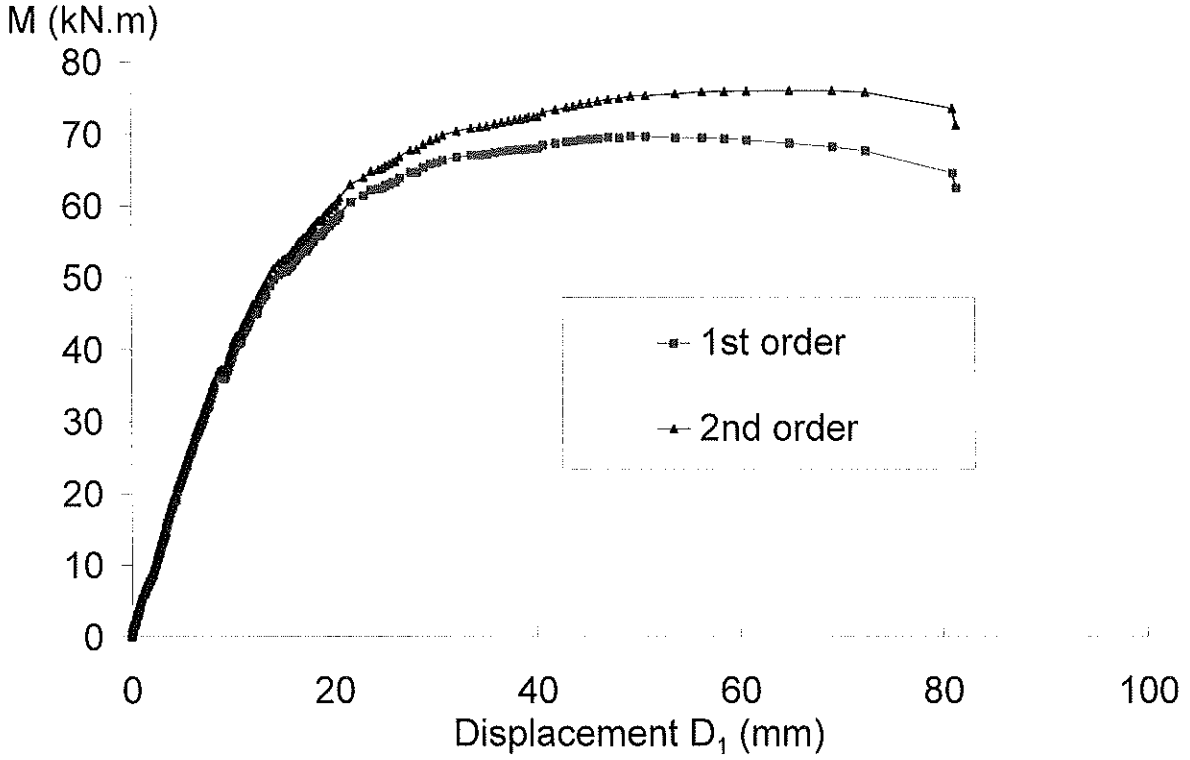

Figure 2.9 - Comparison between the first and second order M-D_1 curves (test PC2.30.1000).

2.4.1.3 Evaluation of the relative rotation.

The most reliable way to evaluate the rotation of the column base is to derive it from the three measurements carried out on the steel profile, i.e. the two rotational transducers ROT_1 and ROT_2 and the displacement transducer D_1. It is obvious that, in addition to the deformation of the column base, these measurements also include the elastic deformation of the column in bending and shear (except for test PC4.30.1000 where the column stub experiences severe yielding; this problem will be discussed later). Figure 2.10 illustrates the deformation of the column stub subject to a transverse concentrated force P.

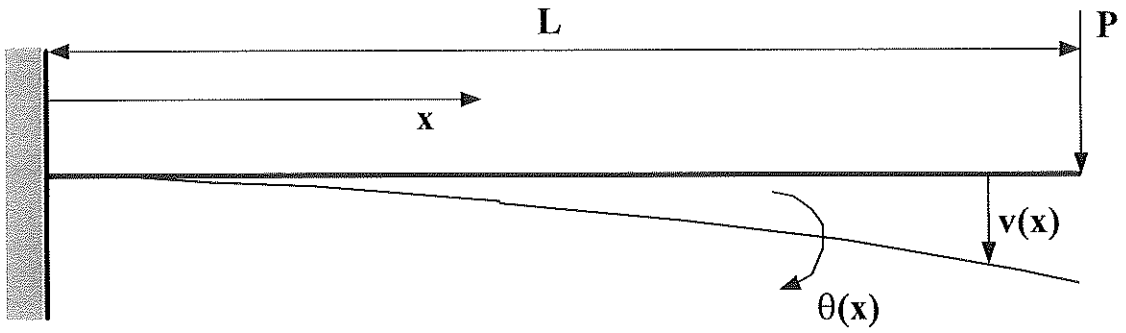

Figure 2.10 - Deformation of the steel column.

The shear deformation of the column stub cannot be ignored because of its limited length and the following expressions are therefore obtained:

$$M(x) = P.(L - x)$$

$$\theta(x) = \frac{P}{E.I}(L.x - \frac{x^2}{2}) \qquad (2.4)$$

$$v(x) = \frac{P}{E.I}(\frac{L.x^2}{2} - \frac{x^3}{6}) + \frac{P}{G.A'}$$

where P = Applied force (Figure 2.10)
L = Length of the element (Figure 2.10)
E = Young's modulus
G = Coulomb modulus (modulus of transverse elasticity)
I = Moment of inertia
A' = Reduced area
v(x) = deflection at one point
θ(x) = absolute rotation at one point

The positive sign of v(x) and θ(x) is indicated by the arrows in Figure 2.10.
On the basis of A' and I characteristics obtained from the actual geometrical properties measured in the laboratory, it is possible to calculate the deflection and the theoretical rotation at any point of the column, and in particular, there where the rotational transducers ROT_1 and ROT_2, as well as the D_1 deflection transducer, are located (Figure 2.7) :

$$v(x=0,9\ m) = 0,063.P\ mm \qquad (2.5)$$

$$\theta(x=0,9\ m) = 0,094.P\ mrad \qquad (2.6)$$

$$\theta(x=0,15\ m) = 0,025.P\ mrad \qquad (2.7)$$

It should be remembered that equations (2.5) to (2.7) are only valid when the column is totally elastic, what is true for all the tests (except for PC.4.30.100 where yielding occurs, at a very advanced stage of loading).

The rotation ϕ of the column base can be now expressed. The rotational transducers constitute the simplest method in the sense that they directly give the desired rotation, provided that the deformation of the steel profile is subtracted. Two different estimations of the same rotation φ may therefore be obtained as follows :

$$\varphi_a = ROT_2 - 0{,}025.F_2(\text{en kN}) \tag{2.8}$$

$$\varphi_b = ROT_1 - 0{,}094.F_2(\text{en kN}) \tag{2.9}$$

These expressions have been derived by substituting P by F_2 in Formulae (2.6) and (2.7), so neglecting the second order effects. In fact, it has been demonstrated that these effects alter in a non significant way the rotations φ_a and φ_b ; for sake of simplicity, it has therefore been decided not to report the "exact" expression of φ_a and φ_b here.

A third estimation may also be calculated from transducer D_1:

$$\varphi_c = \frac{D_1 - 0{,}063.F_2}{0{,}9.10^3} \tag{2.10}$$

Equations 2.8 to 2.10 have been compared for the twelve tests. The similarity is so excellent that it is often impossible to distinguish between the three curves. Thus, in order not to burden the present report unnecessarily, only the curves which have been calculated on the basis of equation (2.8) are included in the next sections.

Before discussing the test results, it is quite important to point out, again, that the M-ϕ curves reported below include the deformation of the column base itself and the possible plastic contribution to the rotational deformation of the column profile close to the base plate.

2.4.2 Comparison of the curves.

Figure 2.11 shows a comparison between the moment-rotation curves for the three tests PC2.15. It has to be noted that, for the tests carried out, the higher the force in the column, the higher the bending moment resistance of the column base.

The initial stiffness of the curves is quite similar for the three tests, as far as the very first loading steps are considered. In fact, the stiffness changes significantly as soon as a separation is observed between the plate and the concrete in the tensile zone. Obviously, the lower the initial compression force the more quickly this phenomenom occurs.

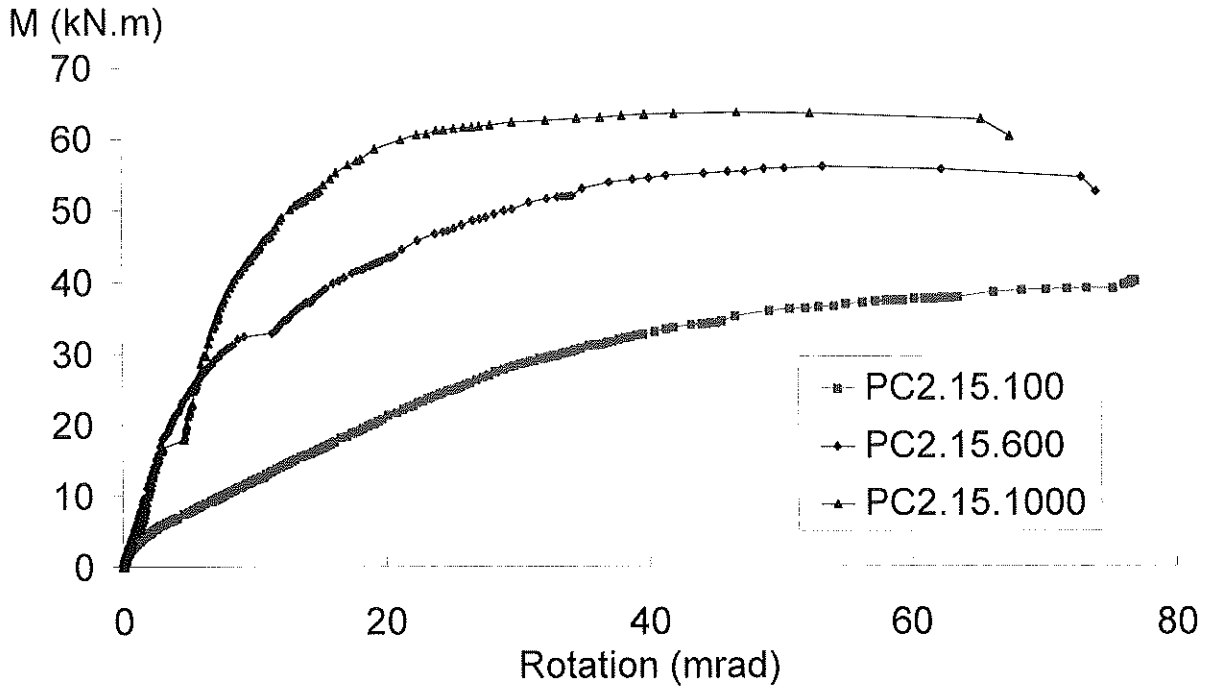

Figure 2.11 - M-φ curves for tests PC2.15.

Figure 2.12 relates to tests PC2.30. Unlike the previous figure, it shows that the initial stiffness of test PC2.30.100 is much lower than that of the other two tests PC2.30. This might be explained as follows: when the blocks were concreted, the anchor bolts embedded in the concrete were held by a plywood board located at the level of the top face of the block and supported by the lateral shuttering. The fresh concrete just arrived at the level of the lower surface of the boards and the concrete was less vibrated then elsewhere, because of the limited accessibility. When it hardened, it proved to be of inferior quality, containing numerous air bubbles. The introduction of a compression force into the column had the effect of homogenizing the concrete located under the plate by reducing its porosity. The higher the compression force, the lower default in the concrete, and the steeper the moment-rotation curve. This could explain the significant difference observed between the curves relating to test PC2.30.100 and the two other tests PC2.30.600 and PC2.30.1000.

By examining Figure 2.11 and Figure 2.12, the particularly high value of the ultimate strength of these column bases, traditionally considered as nominally pinned, can be noted.

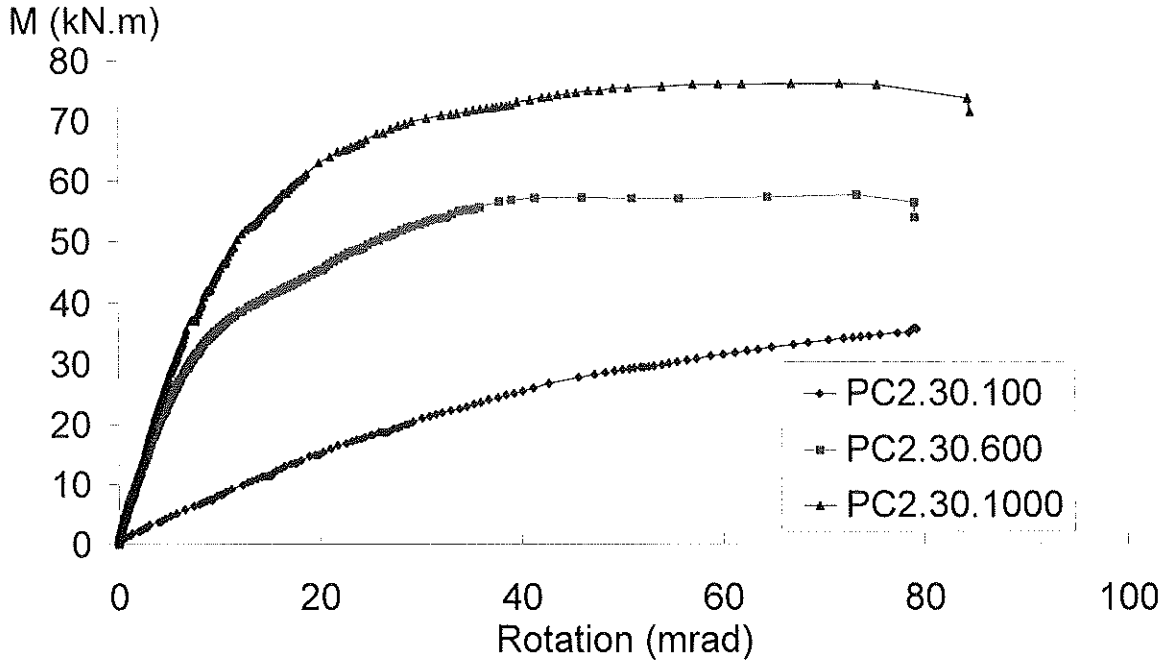

Figure 2.12 - M-φ curves for tests PC2.30.

Figure 2.13 shows the three curves for tests PC4.15. Test PC4.15.400 is the only one which has been subjected to an unloading/reloading cycle.

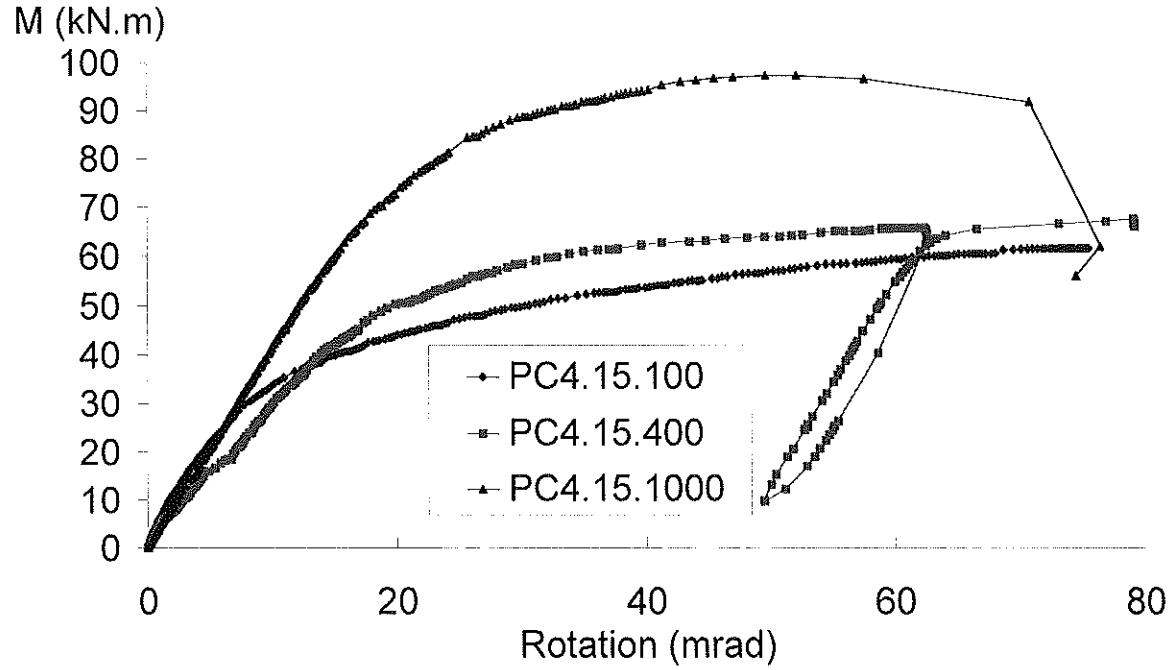

Figure 2.13 - M-φ curves for tests PC4.15.

The very marked difference in strength between test PC4.15.1000 and the other two tests PC4.15 has to be pointed out. This is readily explained by the fact that the anchor bolts in tension are activated much later when the compression force in the column is high.

Finally, Figure 2.14 shows the curves of to the four last tests, PC4.30. These are, a priori, the most rigid and the strongest, what is confirmed by their moment-rotation curves. Unlike the three previous figures it will be noted that test PC4.30.1000 does not reveal a greater strength than test PC4.30.400. In fact, this is due to the yielding of the end section of the steel profile HE160B, as explained later.

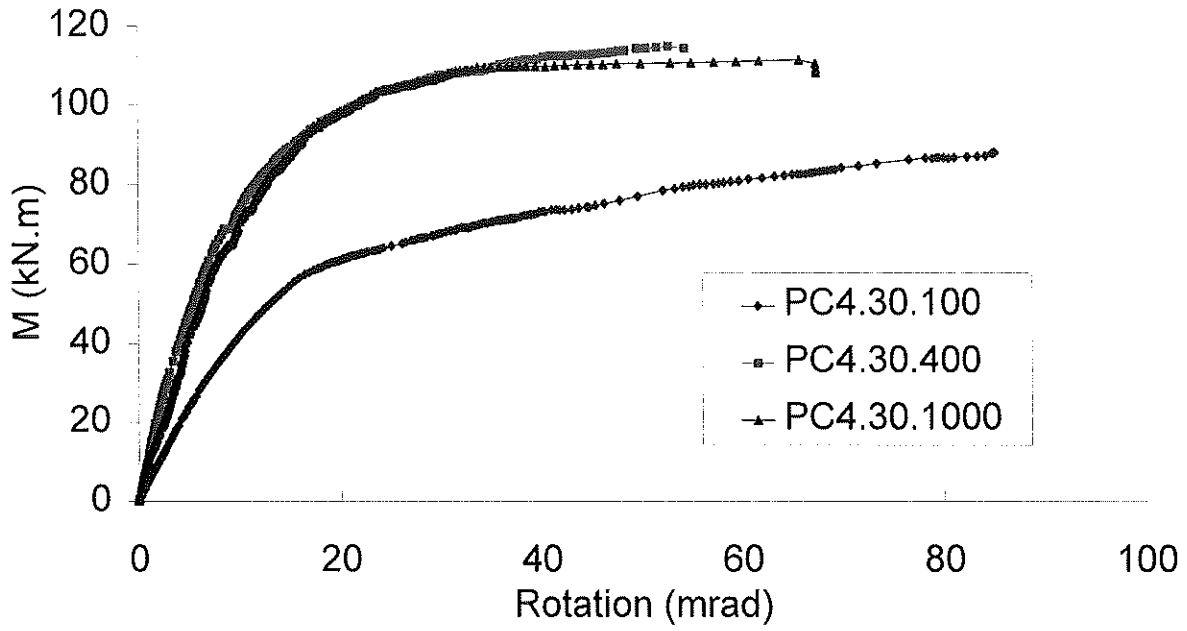

Figure 2.14 - M-φ curves for tests PC4.30.

2.4.3 Main characteristic values of the curves.

Some characteristic values can be derived from the curves shown in Figure 2.11 to Figure 2.14. These will allow comparisons to be made with the theoretical models described later. These quantities are:

- the initial stiffness (slope of the initial part of the curve);
- the ultimate strength: peak value of the M-φ curve;
- the failure mode of the column base.

Table 2.3 presents the measured values of these quantities for each of the twelve experimental tests. $S_{j,ini}$ designates the initial stiffness and $M_{Ru,test}$ the ultimate strength. The value of the pseudo-plastic resistance is not given here because the shape of the curves varies from one test to another. It is very difficult to measure it objectively.

Name	$S_{j,ini}$	$M_{Ru,test}$	Collapse mode
	kN.m/mrad	kN.m	-
PC2.15.100	0.9	40	Failure of anchor bolts
PC2.15.600	5.5	56	Failure of anchor bolts
PC2.15.1000	7	63	Crushing of the concrete
PC2.30.100	0.75	35	Failure of anchor bolts
PC2.30.600	4.6	57	Failure of anchor bolts
PC2.30.1000	5.2	75	Failure of anchor bolts
PC4.15.100	3.5	62	Yielding of the plate
PC4.15.400	4	68	Collapse of the plate and of anchor bolts
PC4.15.1000	4	97	Yielding of the plate
PC4.30.100	4.5	86	Tearing of the anchor bolts
PC4.30.400	11	117	Tearing of the anchor bolts
PC4.30.1000	8	110	Yielding and local buckling of HEB160

Table 2.3 - Characteristic quantities of the experimental tests.

Analysis of Table 2.3 confirms the conclusions previously drawn: the most rigid and resistant tests, for a given configuration, are those for which the compressive force in the column is high. The only exception is test PC4.30.1000 for which considerable yielding of the column cross-section is observed at failure.

Test PC2.30.100 differs from the other twelve tests by a particularly low stiffness and strength. This point has been discussed here above.

3. ANALYTICAL MODEL

In this chapter an analytical model for the prediction of the ultimate and design resistance of column bases with two or four anchor bolts is presented. It is partly based on the revised Annex J and Annex L of Eurocode 3 [2] [3] for what regards the resistance of the components. Despite its simplicity, this model is seen to be in a rather good agreement with the available test results.
The possibility to develop such a model for the evaluation of the initial stiffness is then discussed.

3.1 Evaluation of the resistance.

3.1.1 Introduction

In the following sections, the carrying capacity of the constitutive components is first given. The assembly procedure is then discussed. Finally, comparisons with test results are shown.

3.1.2 Carrying capacity of the concrete block

3.1.2.1 In the case of axial compression

It is relatively simple to calculate the strength of the concrete block under axial compression if the recommendations of Annex L of Eurocode 3 [2] are followed.

The first step consists in calculating a "concentration ratio", k_j, which is dependent on the geometrical dimensions of the block (Figure 3.1.):

$$k_j = \sqrt{\frac{a_1 . b_1}{h_p . b_p}} \tag{3.1}$$

where: h_p = length of the base plate;
b_p = width of the base plate;
a_1 = effective length of the concrete block;
b_1 = effective width of the concrete block.

The effective dimensions of the concrete block, a_1 and b_1, are calculated using the following equations:

$$a_1 = \min(h_p + 2a_R \; ; \; 5\,h_p \; ; \; h_p + h_{block} \; ; \; 5.b_1) \geq h_p \tag{3.2.a}$$

$$b_1 = \min(b_p + 2b_R \; ; \; 5.b_p \; ; \; b_p + h_{block} \; ; \; 5.a_1) \geq b_p \tag{3.2.b}$$

where: a_R and b_R are given in Figure 3.1
h_{block} = height of the concrete block.

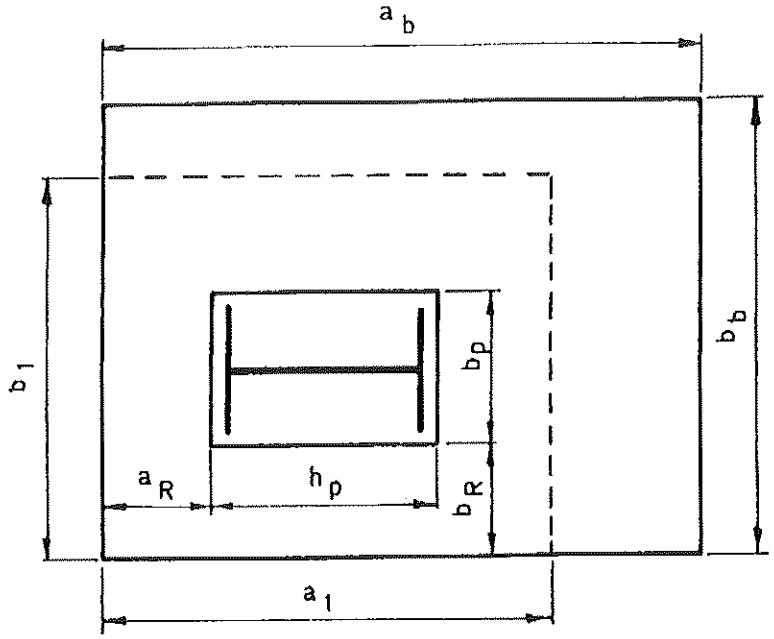

Figure 3.1 - Actual and effective dimensions of the concrete block

The maximum stress that the concrete can resist, f_j, is then evaluated by means of the following equation:

$$f_j = \beta_j . k_j . \frac{f_{ck}}{\gamma_c} \tag{3.3}$$

where: β_j = 2/3 ([1])
f_{ck} = characteristic strength of the concrete in compression
γ_c = partial safety factor for the concrete.

Finally, to take into account the flexibility of the base plate, an equivalent rigid plate (Figure 3.2) is defined, through parameter c given by :

$$c = t_p . \sqrt{\frac{f_{yp}}{3 . f_j . \gamma_{M0}}} \tag{3.4}$$

where: t_p : thickness of the base plate;
f_{yp} : yield strength of the base plate;
γ_{M0} : partial safety factor for steel.

[1] To apply this value, two requirements on the grout layer (between the plate and the concrete) have to be satisfied, what occurs in most of the usual cases.

Obviously, the dimensions of the equivalent rigid plate have not to exceed those of the actual base plate.

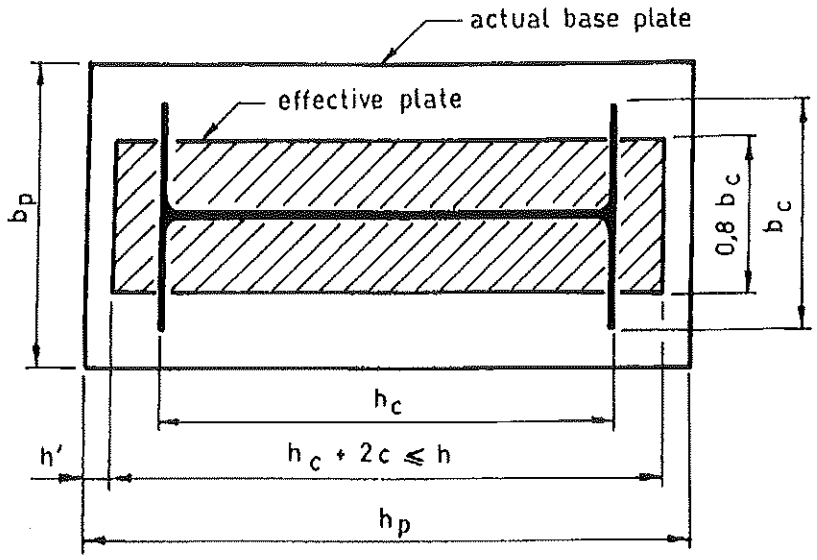

Figure 3.2 - Dimensions of the equivalent rigid plate

Finally the maximum resistance of the concrete block under axial compression is expressed :

$$N_{c,Rd} = f_j . A_{eff} \qquad (3.5)$$

where A_{eff} is the effective area of the equivalent rigid plate defined in Figure 3.2.

3.1.2.2 In the case of non-axial compression

It is obvious that all the developments described in the foregoing paragraph may be used to calculate the carrying capacity of the concrete block under non-axial compression; this is done by considering the effective area defined in Figure 3.2 as being independent on the eccentricity of the applied compressive force.

3.1.3 Strength of the anchor bolts in tension and the base plate in bending

The strength of the whole "plate and anchor bolts" assembly, as a whole, can be determined on the basis of the recommendations given in the Annex J of Eurocode 3 [3]. The calculation is based on the "equivalent T-stub" approach where the actual plate - here the base plate - is replaced by symmetric T-stubs of effective length ℓ_{eff}. The reader is begged to refer to Eurocode 3 revised Annex J for more details about the T-stub approach.

The design resistance $F_{t.Rd}$ of the equivalent stub is the smallest of the resistances obtained by the three following equations :

Mode 1 : plastic yield mechanism in the base plate

$$F_{t,Rd} = \frac{(8.n - 2.e_w).\ell_{eff,1} \cdot m_{pl.Rd}}{2.m.n - e_w(m+n)} \tag{3.6}$$

Mode 2 : mixed failure involving yield lines - but no mechanism - in the plate and exhaustion of the strength of the anchor bolts

$$F_{t,Rd} = \frac{2.\ell_{eff,2} \cdot m_{pl.Rd} + n.\sum B_{t.Rd}}{m+n} \tag{3.7}$$

Mode 3 : failure of the anchor bolts in tension

$$F_{t,Rd} = \sum B_{t.Rd} \tag{3.8}$$

with : $e_W = d_W/4$ (d_W is the diameter of the washer or the nut if there is no washer);

$$m_{pl.Rd} = \frac{t_p^2.f_{yp}}{4.\gamma_{M0}} \tag{3.9.a}$$

where: $m_{pl.Rd}$: plastic moment of the base plate per unit length;
t_p : thickness of the base plate;
f_{yp} : yield strength of the base plate;
γ_{M0} : partial safety factor;
$\ell_{eff,1}$ and ℓ_{eff2} : effective lengths (see below);

$$B_{t.Rd} = 0{,}9\frac{A_s.f_{ub}}{\gamma_{mb}} \tag{3.9.b}$$

where: $B_{t.Rd}$: design resistance of an anchor bolt in tension;
A_s : stress area of the anchor bolts in tension;
f_{ub} : ultimate strength of the anchor bolts;
γ_{mb} : partial safety factor for the anchor bolts;
$n = e \leq 1.25\ m$

m and e are defined in Figure 3.3.

$\sum B_{t.Rd}$ is the sum of the design resistances in tension of all the anchor bolts belonging to the T-stub being considered.

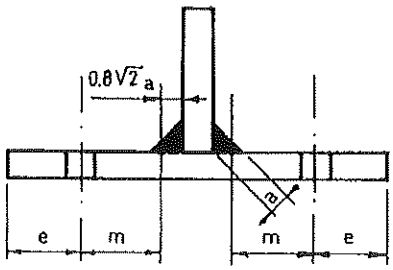

Figure 3.3 - Geometrical characteristics of an equivalent welded T-stub

Two effective lengths $\ell_{eff,1}$ and $\ell_{eff,2}$ are defined for each equivalent T-stub. The first one applies for Mode 1 failure; the second for Mode 2 failure. In fact, according to Eurocode 3, two types of plastic yield mechanisms may occur in plated components, like base plates, subject to transverse forces : circular and non-circular ones. Circular yield line patterns form is the plate without developing any prying effects between the plate and the foundation. The possible failure modes are therefore limited to Mode 1 and Mode 3. In the case of circular patterns, Mode 1, 2 or 3 failures may occur.

As a consequence, $\ell_{eff,1}$ and $\ell_{eff,2}$ are defined as follows :

$$\ell_{eff,1} = \min\left(\ell_{eff,cp}; \ell_{eff,nc}\right) \qquad (3.10.a)$$

$$\ell_{eff,2} = \ell_{eff,nc} \qquad (3.10.b)$$

where $\ell_{eff,cp}$ and $\ell_{eff,nc}$ are the minimum values of the effective lengths associeted to all the yield lines patterns, respectively circular and non-circular, which are likely to develop in the plated component being considered.

For the practical applications, the calculation of the effective lengths is derived from the following formulations:

Anchor bolts located between the column flanges

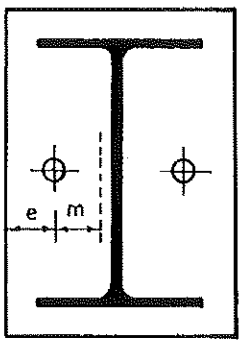

Figure 3.4 - Anchor bolts located between the column flanges

Assuming that bolt row is located at mid-distance between the column flanges, ℓ_{eff} is determined by the following formula:

$\ell_1 = 2\alpha m - (4m + 1{,}25e)$

$\ell_2 = 2\pi m$

$\ell_{eff,1} = \min(\ell_1; \ell_2)$

$\ell_{eff,2} = \ell_1$

where m, n are shown in Figure 3.4 and α is defined in EC 3 Annex J.

Anchor bolts located in the extended part of the plate

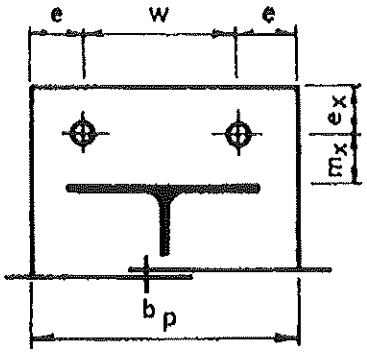

Figure 3.5 - Anchor bolts located in the extended part of the plate.

In this case the effective length is evaluated as follows :

$$\ell_1 = 4.m_X + 1{,}25\, e_X$$
$$\ell_2 = 2\pi\, m_X$$
$$\ell_3 = 0{,}5.b_p$$
$$\ell_4 = 0{,}5.w + 2.m_X + 0{,}625.e_X$$
$$\ell_5 = e + 2.m_X + 0{,}625.e_X$$
$$\ell_6 = \pi m_x + 2e$$
$$\ell_{eff,1} = \min\left(\ell_1; \ell_2; \ell_3; \ell_4; \ell_5; \ell_6\right)$$
$$\ell_{eff,2} = \min\left(\ell_1; \ell_3; \ell_4; \ell_5\right)$$

where b_p, m, e, m_X, e_X and w are given in Figure 3.5.

It has to be noted that these formulae for ℓ_{eff} only apply to base plates where the anchor bolts are not located outside the beam flanges, as indicated in Figure 3.7.

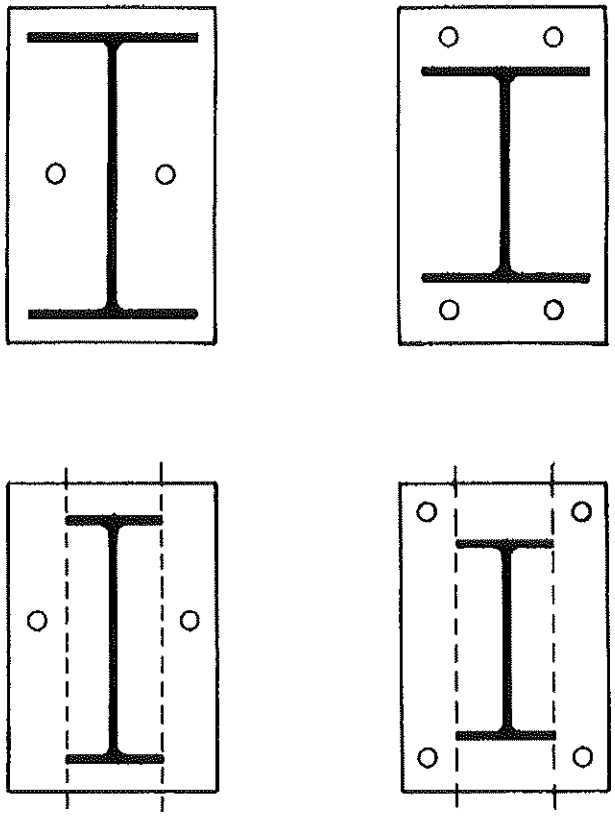

a - Covered b - Not covered

Figure 3.6 - Limits of validity for Formulae (3.6) and (3.7).

The application of the T-stub approach - as recommended in Eurocode 3 Annex J - to column bases possibly requires some adaptations ; these are discussed in section 4.2.2.

3.1.4 Resistance of the steel profile.

The steel column is subjected to combined bending and compression. In the case of HE sections of classes 1 and 2, bent about the strong axis, the bending resistance of the cross-section is expressed by the following equation extracted from Eurocode 3 :

$$M^*_{Rd} = 1{,}11\, M_{pl.Rd}\,(1-\frac{N^*_{Rd}}{N_{pl.Rd}}) \not> M_{pl.Rd} \qquad (3.11)$$

where: $M_{pl.Rd}$: design moment resistance of the cross-section in bending

$N_{pl.Rd}$: design squash load of the cross-section

M^*_{Rd} and N^*_{Rd} : design values of the bending moment and compressive force simultaneously applied to the column base.

3.1.5 Assembly of the components.

In order to draw the interaction curve between the maximum axial compressive force and bending moment which can be simultaneously applied to column base, a static assembly of the components described above is considered. For column bases with four anchor bolts, the bolts located at the compression side are assumed never to be activated.

Depending on the eccentricity of the axial force in the column - the eccentricity is defined as the ratio between the applied bending moment and axial compressive force - two possible cases may occur. They are described hereafter.

Case 1. No anchor bolt is activated

This case will occur when the axis of the anchor bolts is located there where concrete is in compression, i.e. when the compression force acts only with a slight eccentricity (Figure 3.7). In order to verify the overall rotational equilibrium of the column base, the applied forces and the resistant loads must of course be aligned.

By expressing equilibrium along the column axis (Figure 3.7), it is so possible to write:

$$N^*_{Rd} = 0{,}8.b_c.h_{cpr}.f_j = 0{,}8.b_c(h_{eff} + h' - 2.e).f_j \qquad (3.12)$$

where b_c, h_{cpr}, h_{eff} and e are given in Figure 3.7 while f_j designates the strength of the concrete beneath the plate as given by equation 3.3. h', defined as equal to $(h_p - h_{eff})/2$, is shown in Figure 3.2.

This makes it possible to express the eccentricity e as a function of the axial force:

$$e = \frac{1}{2}\left[h_{eff} + h' - \frac{N^*_{Rd}}{0{,}8.b_c.f_j}\right] \qquad (3.13)$$

By introducing (3.13) in (3.12), the value of N^*_{Rd} can be derived. The maximum bending moment which may be applied to the column base together with the compression force N^*_{Rd} is simply obtained by multiplying equation (3.13) by N^*_{Rd}. This approach is valid as long as :

$$h_{cpr} \geq h_{eff} + h' - d$$

where d is the distance between the edge of the plate in the tension zone and the axis of the anchor bolts.

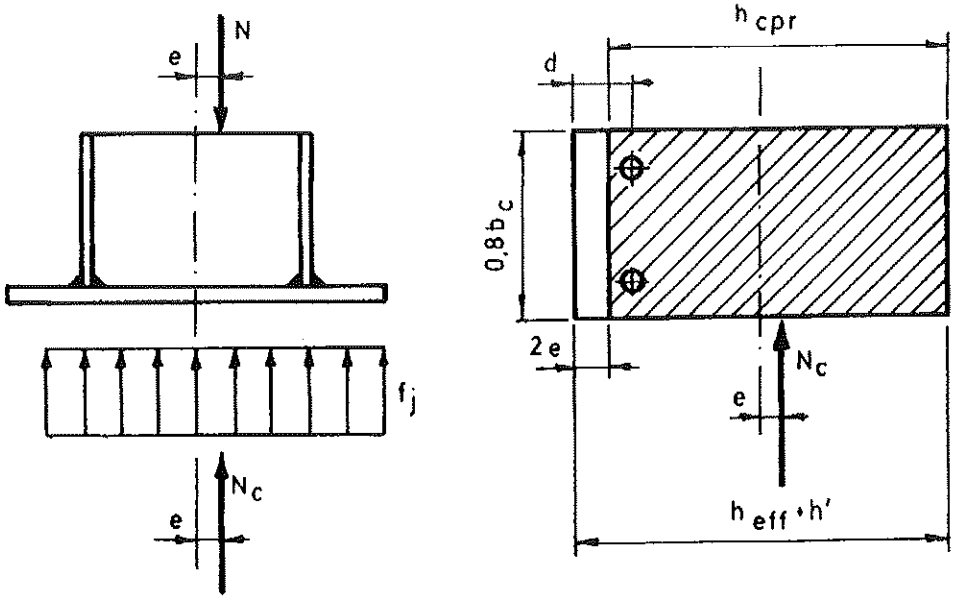

Figure 3.7 - Case 1: Bolts not activated in tension

Case 2. Anchor bolts are actived in tension

As explained in the foregoing paragraph, the anchor bolts are not actived in tension as long as $h_{cpr} \geq (h_{eff} + h' - d)$.

For increasing eccentricities, the value of h_{cpr} decreases, what results in a progressive activation of anchor bolts in tension (force F_b in Figure 3.9).

For a specific value of h_{cpr}, defined as equal to $\zeta(h_{eff} + h' - d)$ hereafter, F_b reaches the tensile resistance $2B_{t.Rd}$ of the row of anchor bolts. For lower values of h_{cpr}, F_b remains than equal to $2B_{t.Rd}$.

The variation law of F_b versus h_{cpr} has been selected as linear on a totally empirical basis. It is represented by equation 3.14 and illustrated in Figure 3.8.

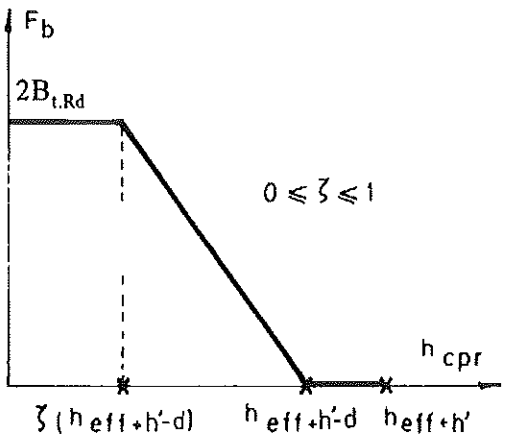

Figure 3.8 - Variation law of F_b

$$F_b = \begin{cases} 0 & \text{si } h_{cpr} \geq h_{eff} + h'-d \text{ (case 1)} \\ 2B_{t.Rd} \cdot \dfrac{(h_{eff} + h'-d) - h_{cpr}}{(1-\varsigma).(h_{eff} + h'-d)} \not> 2B_{t.Rd} & \text{si } h_{cpr} < h_{eff} + h'-d \text{ (case 2)} \end{cases} \tag{3.14}$$

where: h_{eff}: effective height of the plate
h_{cpr}: height of the compressive zone
d: distance between the edge of the plate (tension side) and the axis of the anchor bolts
ζ: parameter varying between 0 and 1. Fixed later.

Thanks to this simplifying assumption, the problem reduces now to the evaluation of h_{cpr} which would result in a distribution of internal forces able to counterbalance the compression force; the maximum eccentricity associated to this force may be deduced.

In fact, from the vertical equilibrium (Figure 3.9) :

$$N^*_{Rd} = 0{,}8.b_c.h_{cpr}.f_j - 2B_{t.Rd}\,\frac{(h_{eff} + h'-d) - h_{cpr}}{(1-\zeta)(h_{eff} + h'-d)} \tag{3.15}$$

$$h_{cpr} = \frac{N^*_{Rd} + 2B_{t.Rd}\,\dfrac{1}{1-\zeta}}{0{,}8.b_c.f_j + 2B_{t.Rd}\cdot\dfrac{1}{(1-\zeta).(h_{eff} + h'-d)}} \tag{3.16}$$

Equation (3.16) is valid only if:

$$\zeta.(h_{eff} + h' - d) \leq h_{cpr} \leq (h_{eff} + h' - d) \tag{3.17}$$

If condition (3.17) is not satisfied and if the conditions relating to case 1 are not fulfilled, then equation (3.16) may be simplified as follows:

$$h_{cpr} = \frac{N^*_{Rd} + 2B_{t.Rd}}{0{,}8.b_c.f_j} \tag{3.18}$$

Once the height of the compressive zone, h_{cpr}, is known, the force to which the anchor bolts are subjected is calculated using equation (3.14). Finally, the maximum moment that the column base is able to transfer is calculated by expressing the rotational equilibrium about the neutral axis of the column (Figure 3.9):

$$M^*_{Rd} = N^*_{Rd}.e = 0{,}8.b_c.h_{cpr}.f_j.\frac{h_{eff} - h_{cpr}}{2} + F_b.(\frac{h_{eff} + h'}{2} - d) \tag{3.19}$$

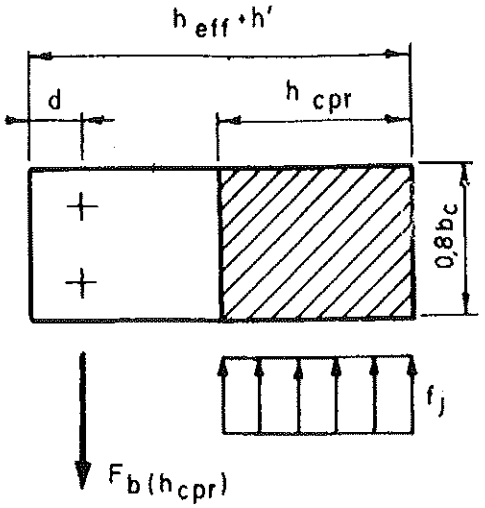

Figure 3.9 - Distribution of internal forces (case 2)

It should be noted that equation (3.19) is also valid when a tensile force is applied to the column, a situation which can occur with light structures subject to strong wind. In the case of column bases with four anchor bolts ("rigid" type), however, it is sometimes necessary to activate the two rows of anchor bolts. For sake of clarity, this situation is not covered here.

The last remaining unknown of the problem is the numerical value to be adopted for the parameter ζ. In reality, this one depends on the mechanical characteristics of the bolts and concrete and, more precisely, on the magnitude of their respective deformations. It is clear that a theoretical evaluation of ζ is quite complex. Thus, for simplicity, its value is fixed empirically. Figures 3.10.a and 3.10.b illustrate the

influence of ζ on the ultimate values N^*_{Ru} and M^*_{Ru} (see annex) of the applied forces in configurations with to 2 and 4 anchor bolts respectively. This influence is seen negligible and a value of 0,5 is thereforeselected for ζ.

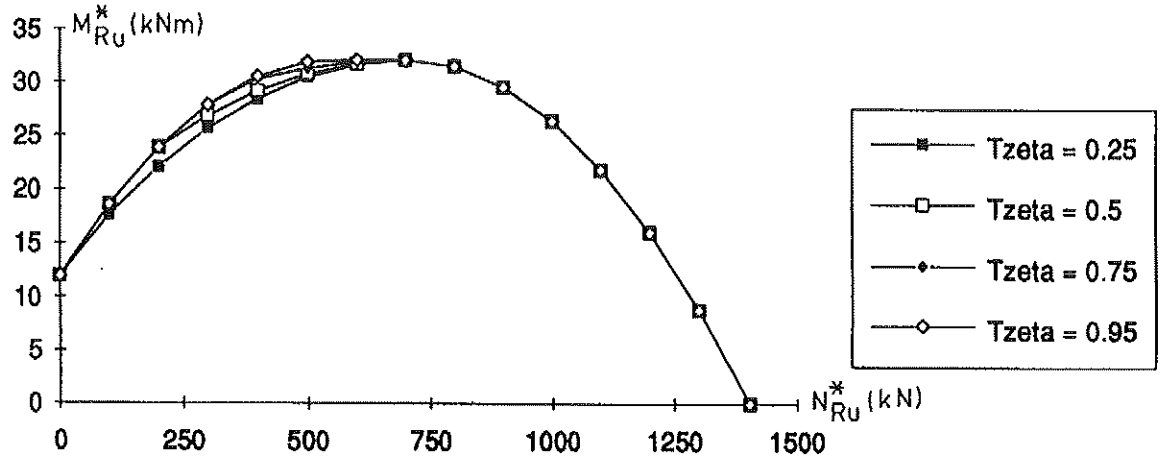

a. Configuration with 2 anchor bolts

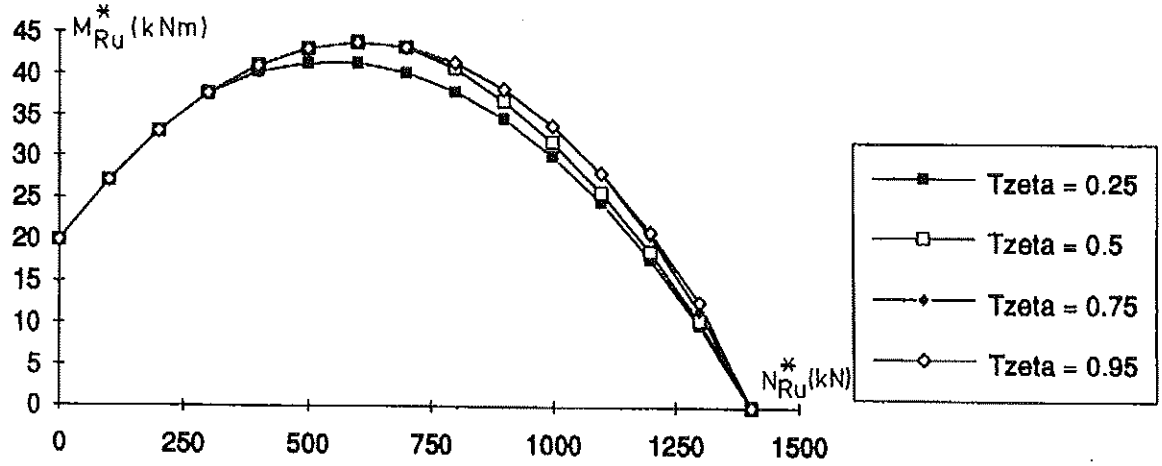

b. Configuration with 4 anchor bolts

Figure 3.10 - Influence of ζ on the ultimate resistance

3.1.6 Comparison with the experimental tests.

Figure 3.11 to 3.15 present a comparison between the analytical model presented in the foregoing paragraphs and the experimental results set out in Table 2.3. The strengths quoted are ultimate ones. It should be remembered that the ultimate load of a column base is calculated by taking into account the ultimate actual strengths of each component (steel, concrete, column cross-section, etc.) and the partial safety factors taken as being equal to unity.

In each of the Figures 3.12 to 3.15, three curves are reported. The first one corresponds to the ultimate resistance of the column base, without any consideration of the possible yielding of the HE160B cross-section (equations 3.12 to 3.19). The second serie of points gives the experimental ultimate strengths reported in Table 2.3. Finally, the last curve covers the carrying capacity of the steel column cross-section considered on its own (equation 3.11).

Tests PC2.15 are reported in Figure 3.11. It is clear that there is an excellent agreement between theory and experimentation. It has also to be noted that the column cross-section is far from experiencing yielding when the collapse of the column base occurs.

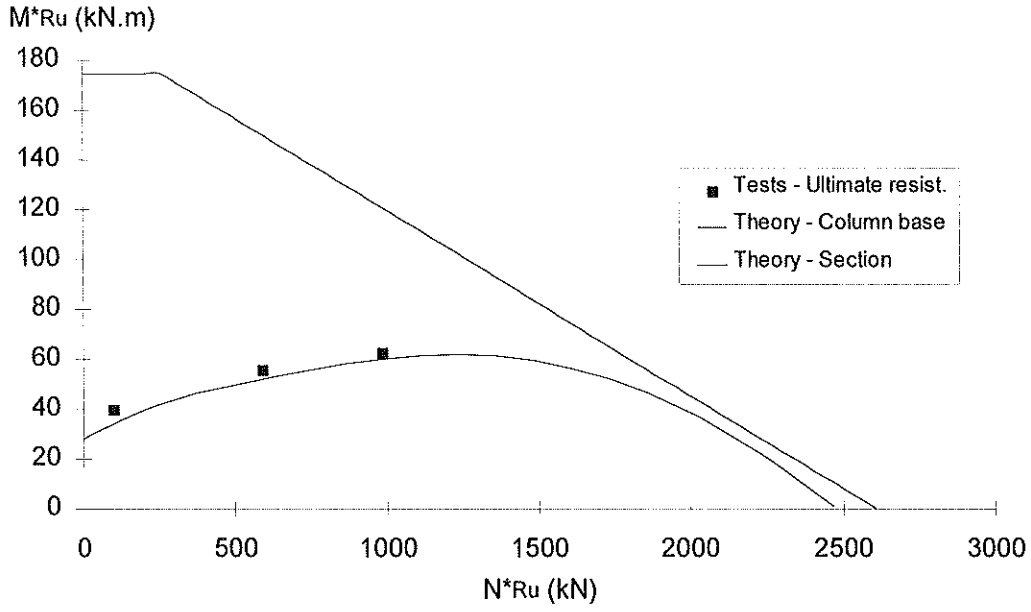

Figure 3.11 - Comparison between tests and model-tests PC2.15

In Figure 3.12, the agreement appears also as satisfactory, even if it is a bit less than in Figure 3.11. The experimental resistance of test PC2.30.100, for instance, is lower than the theoretical prediction. This is due to the fact that the ultimate moment has not been reached during the test which has been interrupted because of high deformations (Figure 2.11).

Nevertheless, bearing in mind the simplicity of the model, the agreement may be considered as quite acceptable.

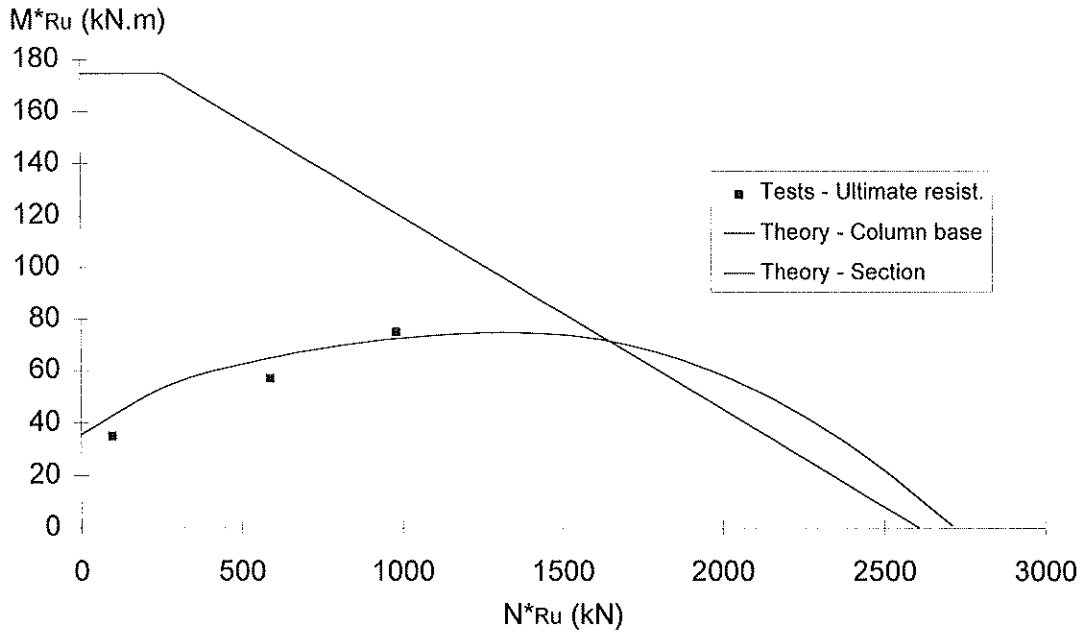

Figure 3.12 - Comparison between tests and model-tests PC2.30

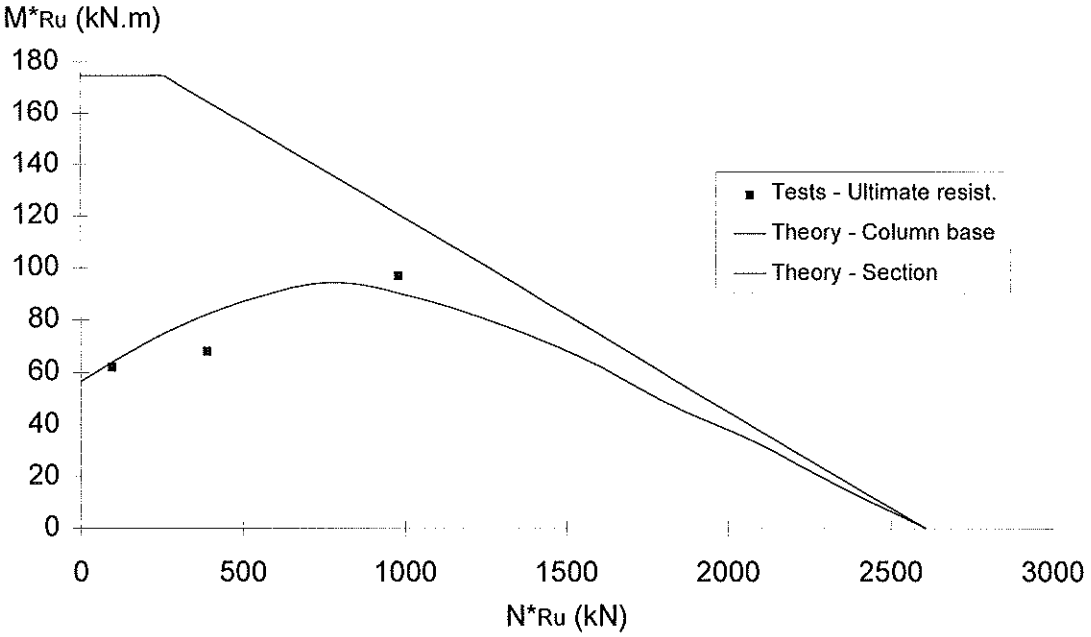

Figure 3.13 - Comparison between tests and model-tests PC4.15

The results for tests PC4.15 are plotted in Figure 3.13. Here again, a rather good agreement between theory and experiment may be seen, except for test PC4.15.400 where, because of its considerable deformability, the peak of the curve has not been reached during the test.

The last serie of tests is presented in Figure 3.14. The agreement between theory and experimentation is again quite acceptable. Test PC4.30.1000 is the only one which fails by lack of resistance of the column cross-section, what is quite in line with what was observed in the laboratory. A slight over-estimation of the strength is noted. That is explained by the local buckling occurring at the end of the test in the column flange in compression. This failure load is not taken into consideration as far as now in the model.

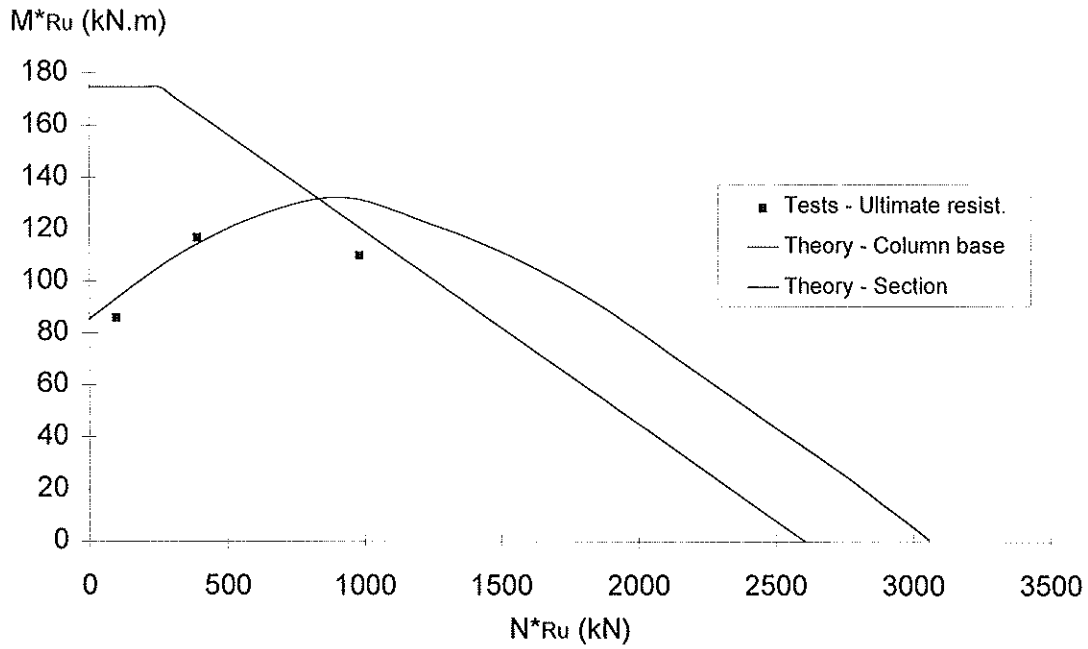

Figure 3.14 - Comparison between tests and model-tests PC4.30

In conclusion, it can be stated that the analytical model, despite its simplicity, is particularly suitable for the prediction of the failure load of column bases.

3.2 Evaluation of the initial stiffness.

The initial stiffness, i.e. the slope of the moment-rotation curve at the origin, is another main mechanical property of the column bases.

By contrast with the beam-to-column joints or beam splices, the initial stiffness of the column bases is difficult to evaluate. The effect of the axial force in the column and the plate-to-concrete contact which involves separation effects, activation or non-activation of the anchor bolts, etc., have to be considered to explain the particular behaviour of column bases. For the test configurations for which the axial applied force is low, a highly premature separation of the plate is observed, what modifies the distribution of internal forces and therefore the global stiffness of the column base. Consequently, by contrast with conventional joints which exhibit an elastic linear initial behaviour, the column bases may experience very quick changes of stiffness. In this context, the need for the theoretical prediction of the initial stiffness becomes questionable.

This is why it has been decided in Liège not to go further with investigations on initial stiffness but to develop a kinematic (mechanical) model allowing to follow the behaviour of the column bases all along their loading history. Such an approach appears as the most suitable one to understand deeply the complex phenomena to which the scientist is faced when studying column bases. We are so following the approach initiated some years ago by Penserini [5], whose works constituted a quite valuable reference all along our developments.

It should be mentioned, however, that the team of F. Wald, in Prague, is actively working on the development of a simple model which should enable the stiffness and strength of column-bases to be evaluated by hand [4].

The combination of these two complementary works in the future could probably help in deriving simple guidelines for practitioners, to be possibly included in a new issue of Eurocode 3 Annex J and L.

4. MECHANICAL MODEL

4.1 Background of the model.

The main objective is to develop a model based on the component method and able to follow the behaviour of the column bases all along their whole range of loading.
To ensure the suitability of the models with the expectations, it appears quite important to take good note of the following observations made during the tests in laboratory :

- The unilateral contact between the plate and the concrete is a complex phenomenon which needs to be described in very refined way.

- The bond between the anchor bolts in tension and the concrete which surrounds them is broken very prematurely, as soon as the anchor bolts are subjected to tension. It is therefore allowed to consider that the bolts are free to elongate over their whole length L_b, as measured from the origin of the curved part up to the mid-thickness of the nut, i.e. approx. 250 mm (see Figure 2.4).

- Under the column flange(s) in compression, the plate undergoes substantial deformations. The pressure under the plate is therefore far from being uniform, even under pure compression. As a consequence, it is absolutely essential to keep the concept of equivalent rigid plate in the model.

- In the compressive zone, the extended part of the steel plate has an essential role as it prevents premature crushing into the concrete. The formation of a yield line in the extended part of the plate all along the column flange can also be noted. This requires substantial deformation energy which ought therefore to be modelled.

- The steel column cross-section experiences yielding which, in some cases, produces significant deformations. To compare the mechanical model with the experimental moment-rotation curves defined in chapter 2 - where the plastic deformations of the cross-section are included - it is absolutely essential to consider these deformations in the model.

- The distribution of the internal forces in a column base changes considerably during its loading. In particular, the contact zone, and therefore the lever arm of the internal forces, are in constant evolution. Furthermore, the individual response of each component (concrete, anchor bolts, plate, section, etc.) is highly non-linear. Therefore only an iterative approach can efficiently describe the behaviour of the column bases throughout the whole loading.

In the light of the above statements and after several trials, which are not described here ; a mechanical model has been finally selected, it is illustrated in Figure 4.1.

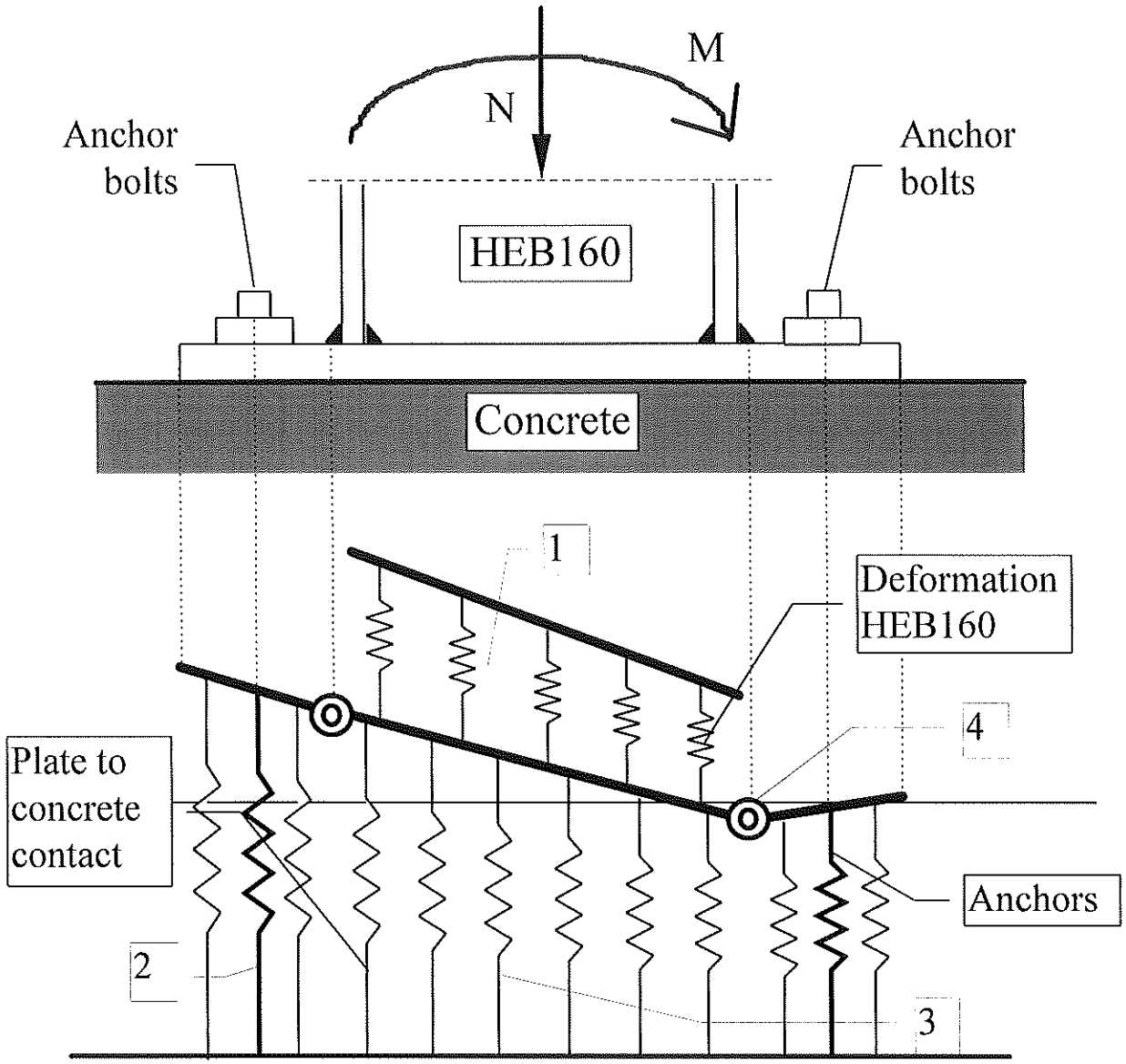

Figure 4.1 - Mechanical model for column bases

In this figure, the following components may be identified:

- Extensional springs to simulate the deformation of ***the column cross-section*** **(1).** These springs work both in tension and compression.
- Extensional springs to simulate the deformation of ***the "anchor bolts and base plate" component*** **(2).** They work only in tension. A single spring is used to model a row of anchor bolts and the corresponding part of the plate.
- Extensional springs to simulate ***the concrete under the plate*** **(3).** They work only in compression.
- Rotational springs used to model the plastic deformation associated to the possible development of a yield line in the extended part of the plate in the compressive zone **(4).** These springs are not activated when the extended part of the plate is in the tensile zone and is therefore no longer in

contact with the concrete as the deformability of the plate is already taken into account in the extensional springs (**2**) aimed at modelling the anchor bolts and plate assembly in the tensile zone.

In the next sections, details about the laws governing the behaviour of these components and the method used to assemble the components together so as to derive the overall response of the whole column base are presented.

4.2 Response of the individual components.

4.2.1 Concrete in compression.

The plate-to-concrete contact is a particularly complex phenomenon because of the modification of the contact zone with the eccentricity of the compressive force and with the flexibility of the plate, which is directly related to its thickness.

First of all, so as to avoid to take explicitly into account the actual flexibility of the plate, the concept of **the equivalent rigid plate**, already discussed in §3.1.2, is used. However, contrary to the static model developed in chapter 3, the purpose of which was to calculate the strength of the column base, the whole loading range, characterized by a substantial variation of the eccentricity of the axial force, is considered here. Thus the choice of a rectangular equivalent rigid plate was no longer suitable at all for describing some ranges of eccentricity. Therefore, the idealization of the plate illustrated in Figure 4.2 is adopted. It is quite close to that recommended in Annex L of Eurocode 3 [2].

The parameter "c" is the one calculated by Formula 3.4. As previously mentioned, yield line(s) are likely to occur in the extended part of the plate. They are located close to the weld, at a distance $0.8.\sqrt{2}.a_f$ of the column flange, where a_f designates the throat radius of the weld between the column flange and the base plate.

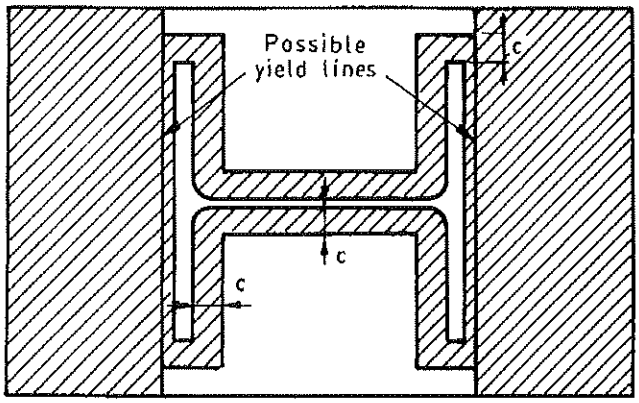

Figure 4.2 - Definition of the equivalent rigid plate for the mechanical model

The law σ-ε adopted for concrete in the model is a conventional parabola-rectangle one, as illustrated in Figure 4.3. It is characterized by an almost straight parabolic part. In fact, this is understandable because the strength f_j (see Formula 3.3) of the concrete takes into account the beneficial effects of the

confinement and is therefore much higher than that measured on cubes. This does not apply to the Young's modulus E_b of the material. In fact, it may be assumed that the confinement only appears when the deformations are significant.

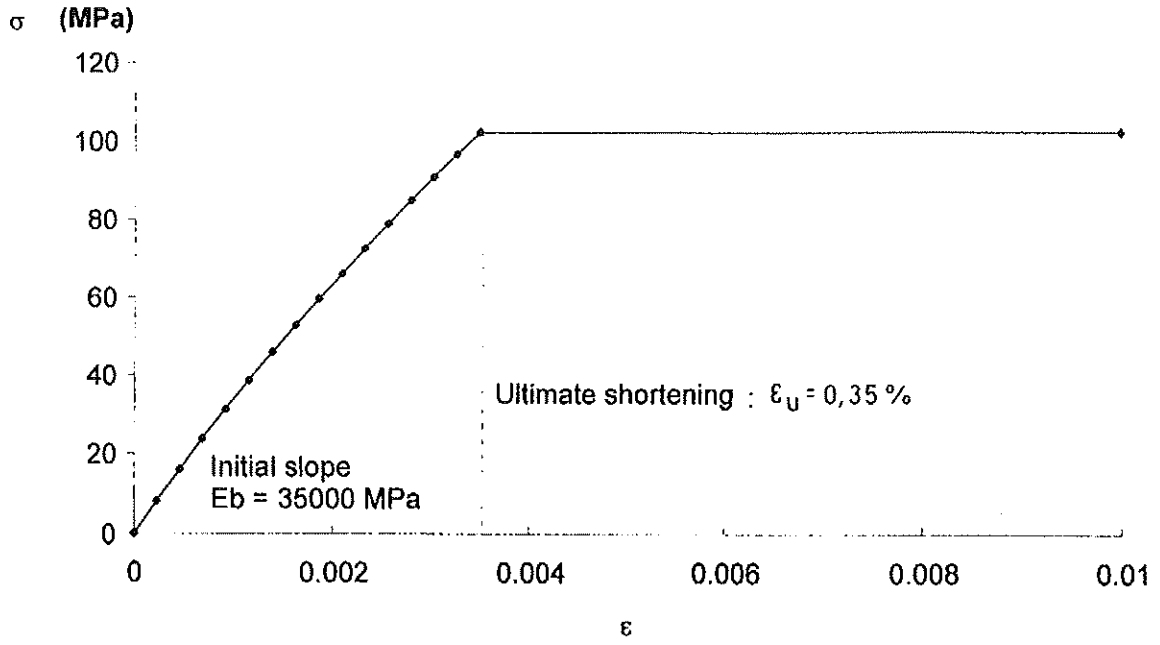

Figure 4.3 - σ - ε law for concrete in compression

Equation 4.1 gives the mathematical expression of the law illustrated in Figure 4.3. The curve passes through the origin, with an initial slope equal to the Young's modulus, and passes through the point (ε_u, f_j).

$$\sigma(\varepsilon) = \frac{f_j - E_b.\varepsilon_u}{\varepsilon_u^2}.\varepsilon^2 + E_b.\varepsilon \qquad (4.1)$$

The concrete-to-plate contact is discretized through the use of a finite number of springs, each covering a small part of the contact zone. A number of preliminary tests have shown that about hundred springs provide sufficient accuracy for discretization. To establish the $F_i - \delta_i$ law of a particular spring, it is sufficient to comply with the two following equations:

$$\begin{aligned} F_i &= \sigma.\Omega_i \\ \delta_i &= \varepsilon.h_{block} \end{aligned} \qquad (4.2)$$

where F_i is the force in the spring i, Ω_i the concrete area it represents, δ_i its elongation; h_{block} is the depth of the concrete block. By combining equations (4.1) and (4.2), the $F_i - \delta_i$ relationship is derived as follows :

$$F_i(\delta_i) = \Omega_i.\left[\frac{f_j - E_b.\varepsilon_u}{\varepsilon_u^2}.\left(\frac{\delta_i}{h_{block}}\right)^2 + E_b.\left(\frac{\delta_i}{h_{block}}\right)\right] \qquad (4.3)$$

Equation 4.3 is based on the assumption that the deformation at a point of the plate-to-concrete contact zone is constant over the depth of the block, what is just, of course, a simplification. However, for reasonable dimensions of the block, what is the case for the tests considered here, this idealization gives similar results than those supplied by more complex models, as the PENSERINI one [5].

4.2.2 Anchor bolts in tension and base plate in bending.

Contrary to the behaviour of the concrete which is identical for each of the twelve tests, the curve relating to the "anchor bolts in tension and plate in bending" assembly depends (a) on the thickness of the plate and (b) on the position of the row: between the flanges or outside the flanges.
The pseudo-plastic and ultimate resistances of the "anchor bolts-base plate" assembly, respectively termed $F_{Rp,model}$ and $F_{Ru,model}$ (see annex), are given in Table 4.1. They have been basically derived through the use of the formulae given in sections 3.1.3 but sometimes amended as explained in the next paragraphs. As mentioned previously, the ultimate tensile resistance of the anchor bolts has not been reached, in the tests presented in Chapter 2, by failure in the cross-section, but by unbending of the curved part. The associated ultimate value measured in laboratory is also reported in Table 4.1 where the italic and bold characters are used for values exceeding $2B_{t,Ru}$.

	PC2.15	PC2.30	PC4.15	PC4.30
$F_{Rp,model}$ (kN)	327	***1306***	91	363
$F_{Ru,model}$ (kN)	***480***	***1922***	264 (PC4.15.100) 133 (others)	***447*** (PC4.30.100) ***534*** (others)
$2B_{t,Ru}$ (kN)	375			

Table 4.1 Strengths of the anchor bolts and plate in tension.

During the tests, the anchor bolts elongate usually in a significant way, and more particularly in comparison with the deformation of the base plate. As a consequence, prying effects may not develop as they would do in usual end-plate connections. Such a behaviour has been systematically noted in the first loading steps, i.e. there where the response of the column base is approximatively elastic. This explains why the elastic stiffness of the "anchor bolts - base plate" assembly is evaluated below on the basis of a "no prying" situation. For what regards the pseudo-plastic resistance of the "bolt-plate" assembly, a first distinction has to be made between column bases with two and four anchor bolts respectively.

In column bases with two anchor bolts, no prying forces develop all along the loading. Mode 2 failure in the base plate is therefore not contemplated and only circular patterns are likely to contribute to Mode 1 (see Section 3.1.3).

In column bases with four anchor bolts, a similar response is reported for tests PC4.15.100 and PC4.30.100. For the other tests (PC4.15.400 and 1000 and PC4.30.400 and 1000) no prying develops

until the pseudo-plastic resistance of the base plate is reached. But because of the high axial compression force acting in the column, the displacements remain limited in the tension zone and a contact progressively develop between the plate and the concrete when the loading is increased beyond the pseudo-plastic resistance of the column base. Formulae (3.6) to (3.8) are therefore used at ultimate state.

This justifies the different values reported in Table 4.1 according to the test numbers.

For the mechanical model, the whole deformability curve of the "anchor bolts-plate" assembly must be determined. First, the elastic stiffness of the different components is evaluated according to Eurocode 3 Annex J where the force -displacement relationship for each component in the elastic range, is expressed as follows :

$$F = E\,k\,\delta \qquad (4.4a)$$

or $$F = K\,.\,\delta \qquad (4.4b)$$

with : k = stiffness coefficient of the component

K = stiffness of the component

For a row with two anchor bolts, the stiffness coefficient is as follows :

$$k_b = \frac{2.A_s.E}{L_b} \qquad (4.5)$$

where A_s represents the stress area of the anchor bolt, E the Young's modulus for steel and L_b the free length of the bolts. The value to give to L_b has been defined in Section 4.1.
The deformability resulting from the bending of the base plate has to be added to that of the anchor bolts. The elastic stiffness of the base plate is given by :

$$k_p = \frac{E.\ell_{eff}.t_p^3}{2.m^3} \qquad \text{for configurations with 2 anchor bolts} \qquad (4.6a)$$

$$k_p = \frac{E.\ell_{eff}.t_p^3}{2.m_x^3} \qquad \text{for configurations with 4 anchor bolts} \qquad (4.6b)$$

where ℓ_{eff}, m and m_x are given in §3.1.3; t_p is the thickness of the plate. Formulae (4.5) and (4.6) differ from those recommended in revised Annex J because of the absence of prying forces was assumed.

When the elastic stiffness and the resistance of the two components are known, deformability curves for anchor bolts and plate can then be built. Let us start with the anchor bolts in tension. Their behaviour is modelled in accordance with the law illustrated in Figure 4.4. The format of this law is similar to that used in EC3 Annex J but it is referred here, for what regards the peak value of the curve, to the ultimate resistance of the anchor bolts and not to the design resistance as it should be according to Annex J. This freedom has been taken after that the suitability of the proposed law had been checked through comparisons with results of laboratory tests on anchor bolts in tension.

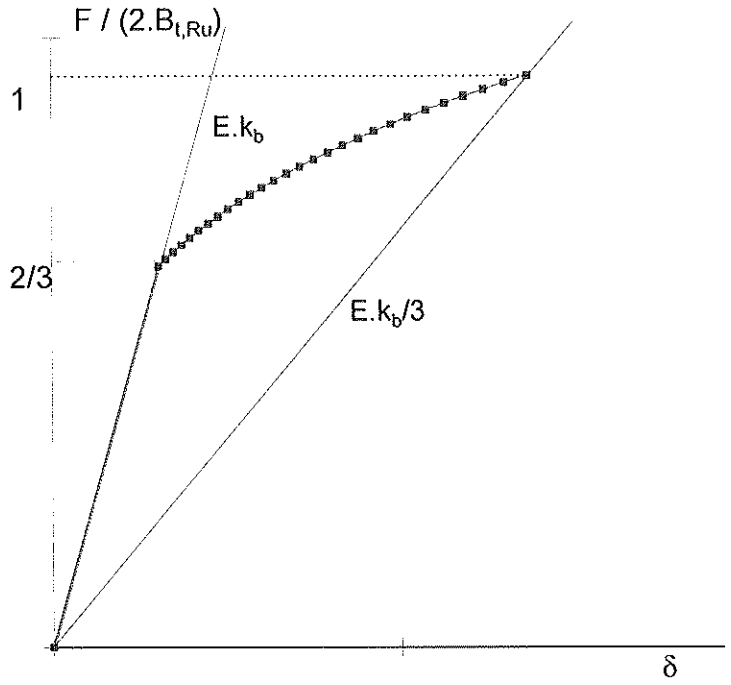

Figure 4.4 - Behaviour law for anchor bolts in tension

The equation of the curve plotted in Figure 4.4 can be expressed as follows:

$$\begin{cases} F = E \,.\, k_b \,.\, \delta & \text{for } F \le \dfrac{2}{3} \,.\, 2\, B_{t.Ru} \\ F = E \,.\, k_b \left(1{,}5 . \dfrac{F}{2\, B_{t.Ru}} \right)^{-2{,}7} \,.\, \delta & \text{for } \dfrac{2}{3} \,.\, 2\, B_{t.Ru} < F < 2\, B_{t.Ru} \end{cases} \qquad (4.7)$$

where $2\, B_{t.Ru}$ designates the ultimate resistance of an anchor bolt row and k_b its elastic stiffness coefficient as given by equation 4.5.

The plate behaviour in bending is modelled in a more complex manner than that of the bolts. Use is made in fact of a model proposed in [6] by the senior author; this one is much more suitable for the modelling of a steel component such as the plate. The F-δ relationship is given by the equation (4.8) :

$$F = \frac{E \,.\, (k_p - k_{p,post-limit}).\delta}{\left[1 + \left[\dfrac{E \,.\, (k_p - k_{p,post-limit}).\delta}{F_{Rp}} \right]^c \right]^{\frac{1}{c}}} + E \,.\, k_{p,post-limit} \,.\, \delta \le F_{Ru} \qquad (4.8)$$

where k_p is the initial stiffness coefficient (equation 4.6) and $k_{p,post-limit}$, the post-limit stiffness coefficient. According to [6], $k_{p,post-limit}$ may be taken equal to 1/40 times the initial stiffness coefficient k_p in the case of column bases with two anchor bolts, and to 1/20 times k_p in the case of column bases with four anchor bolts where the extended part of the base plate experiences larger deformations resulting in the development of membrane effects. F_{Rp} is the pseudo-plastic resistance of the "bolt-plate" assembly and F_{Ru} its ultimate resistance (Table 4.1). Parameter c is a shape factor which has been chosen equal to 1.5 on the basis of comparisons with the experimental data. This value is nothing else than that which is recommended in [6] for most current types of steel beam-to-column joints.

The "anchor bolts + plate" behaviour curve is finally obtained by adding the two "anchor bolts" and "plate" curves (equations 4.7 and 4.8). Figure 4.5 to Figure 4.8 present the resultant curves obtained for the four test configurations described in chapter 2.

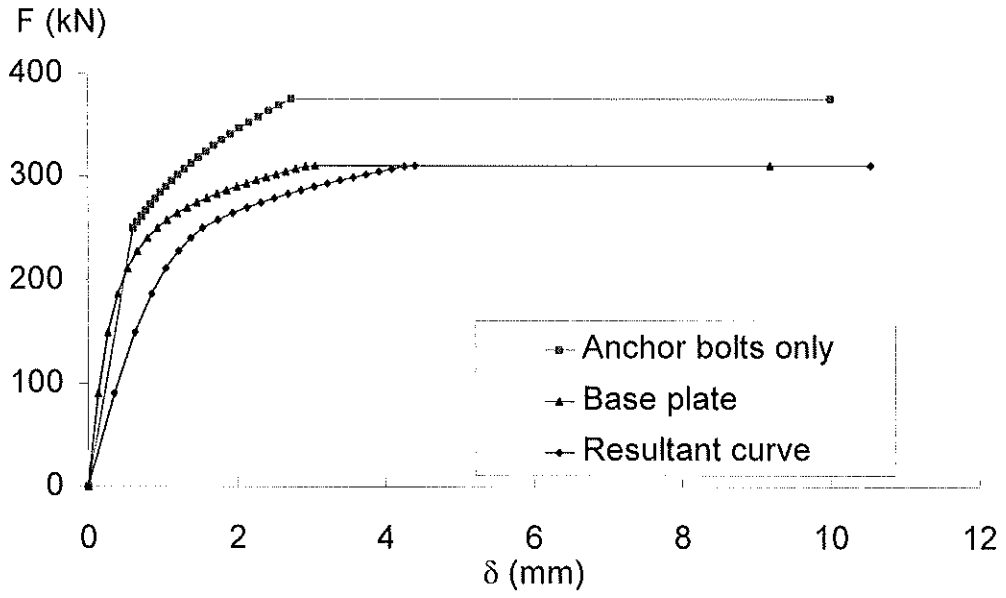

Figure 4.5 - Behaviour law for the "anchor bolts + plate" component. Tests PC2.15

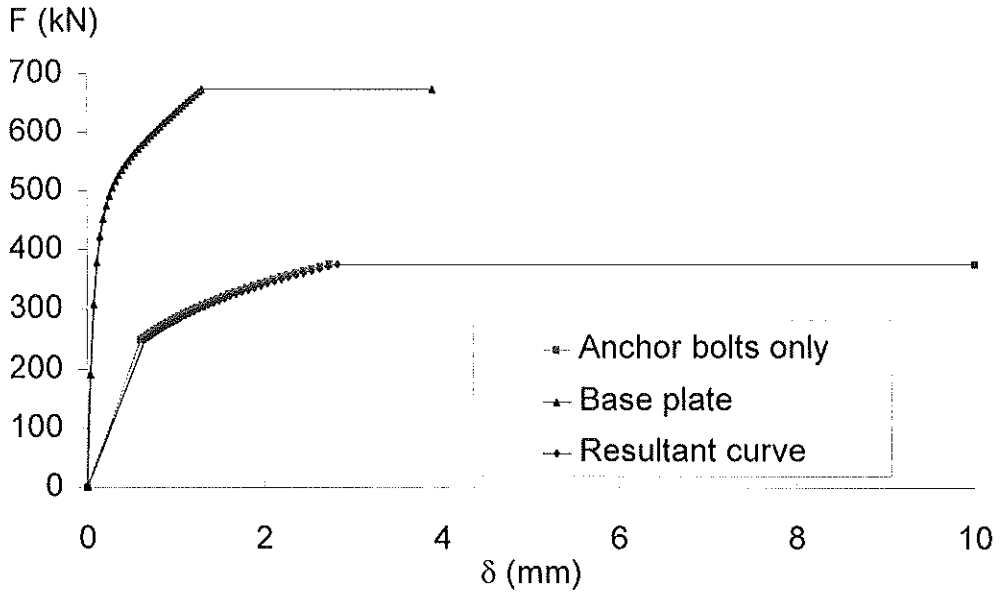

Figure 4.6 - Behaviour law for the "anchor bolts + plate" component. Tests PC2.30

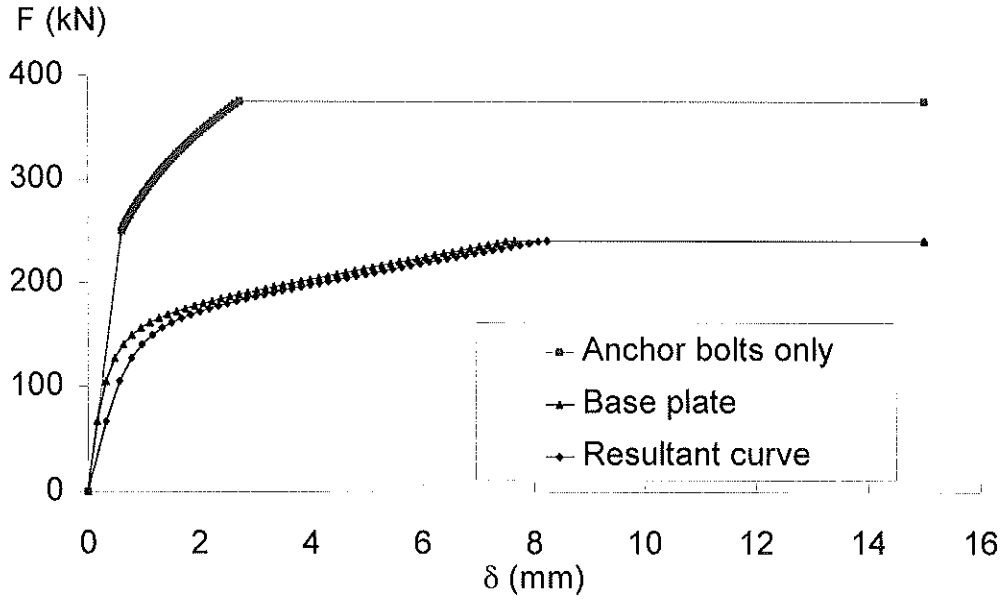

Figure 4.7 - Behaviour law for the "anchor bolts + plate" component. Test PC4.15.100

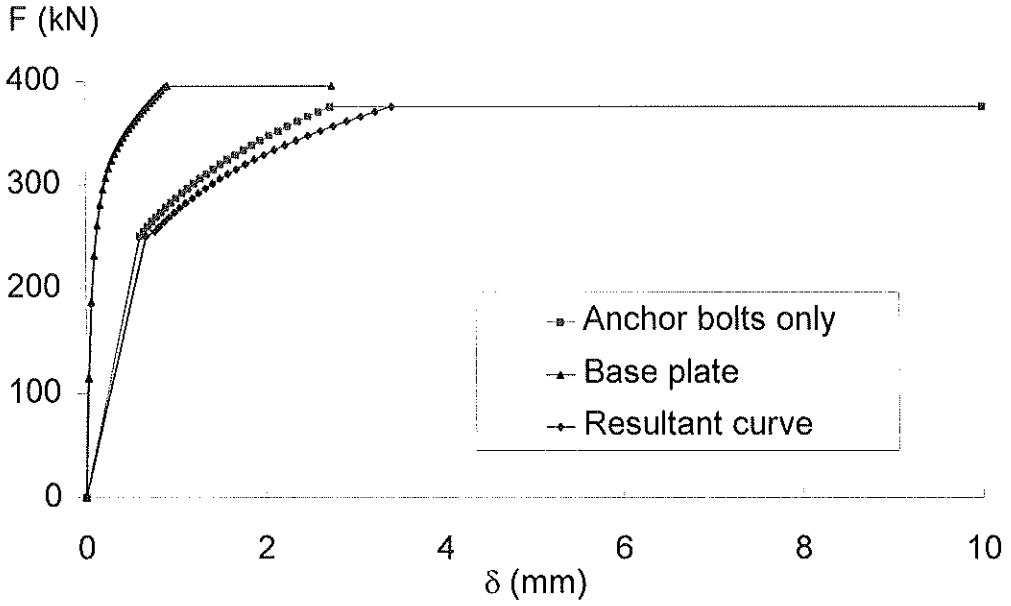

Figure 4.8 - Behaviour law for the "anchor bolts + plate" component. Test PC4.30.100

In addition to the "anchor bolts + plate" deformability in the tensile zone, the plate is also likely to deform in the compressive zone in the case of column bases with four anchor bolts (see Section 4.1). The tests have shown that this deformation is very localized and may be concentrated in a plastic hinge. Thus, in the mechanical model, this deformability is accounted for by means of a rotational spring characterized by an elastic-perfectly plastic law. In the tensile zone, the deformability of the plate is already considered through the above-described "anchor bolts + plate" spring. The stiffness of the rotational spring is therefore taken as infinite in the tensile zone ($K_t = \infty$).

Figure 4.9 illustrates the behaviour law finally adopted.

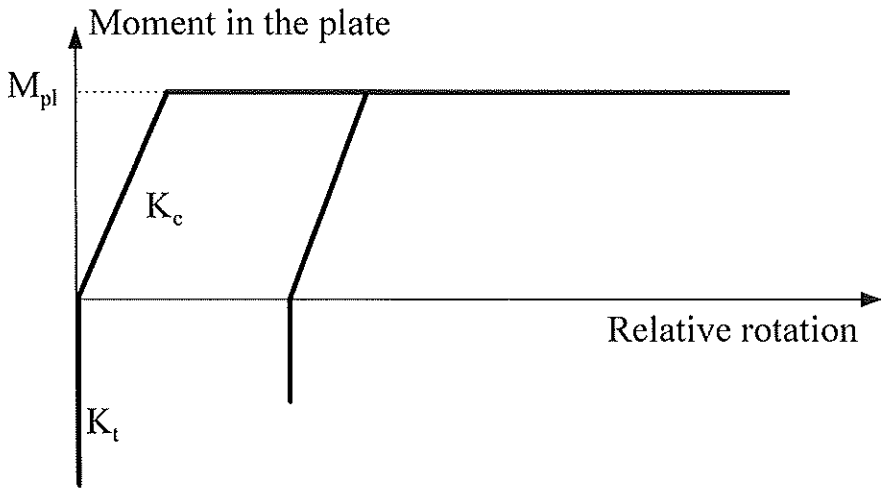

Figure 4.9 - Behaviour law for the plate rotational spring (configuration with four anchor bolts).

The characteristics of the spring, i.e. M_{pl} and K_c, should be evaluated as follows:

$$K_c = \frac{E.b_p.t_p^3}{12}.\frac{1}{t_p} = \frac{E.b_p.t_p^2}{12} \tag{4.9}$$

$$M_{pl} = \frac{b_p.f_{yp}.t_p^2}{4} \tag{4.10}$$

where b_p is the total width of the plate, f_{yp} its yield strength, and t_p its thickness. The calculation of the rotational stiffness (4.9) is based on the assumption that the deformation zone extends over a length equal to the thickness of the plate. However, application of the model to tests has shown that equations (4.9) and (4.10) over-estimate the deformation energy of the plate. In fact, the best agreement has been obtained by giving to K_c and M_{pl} zero values, i.e. the characteristics of a perfect hinge. This assumption has therefore been selected.

4.2.3 Steel profile.

In chapter 2, it has been explained that the column steel profiles HE160B experiences, in some cases, high stresses, what leads to partial yielding of the cross-section. For test PC4.30.1000, a plastic hinge forms, causing the full yielding of the column cross-section.
In order to take this into account in terms of both strength and deformability, the steel cross-section is represented by means of a number of extensional springs, what makes it possible to simulate the development of yielding in the section with increasing values of the bending moment and compressive force.
Figure 4.10 illustrates the way in which the cross-section has been discretized in the mechanical model.

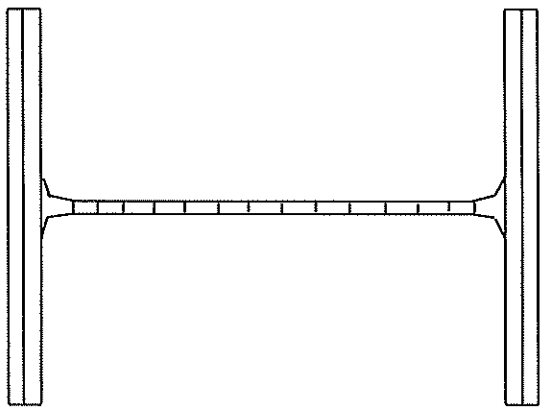

Figure 4.10 - Discretization of the column cross-section for the mechanical model

To each of the small discretized parts of the section represented in Figure 4.10 is associated an extensional spring, the stiffness and strength of which are proportional to the area of this zone. The behaviour law for the constitutive steel is elastic - perfectly plastic. The length of the springs is taken

equal to the distance between the end-plate and the location of the rotational transducer ROT_2 used in laboratory (§ 2.4.1), so as to allow a direct comparison between test and model. An unconsistency is however likely to occur as the elastic contribution to the rotational deformation of the column close to the column base has been withdraw from the experimental M-ϕ curve. As this contribution is seen to be quite negligible, the comparisons may be anyway considered as valid.

4.3 Assembly procedure.

The characterization of the individual behaviour for all the components is followed by the assembly; this one is performed in accordance with the model illustrated in Figure 4.1 where it is assumed, conventionally, that all the vertical forces and moments are positive if they act upward and in the anti-clockwise direction respectively. The same rule applies also to the displacements.
A schematic representation of the model is given in Figure 4.11.

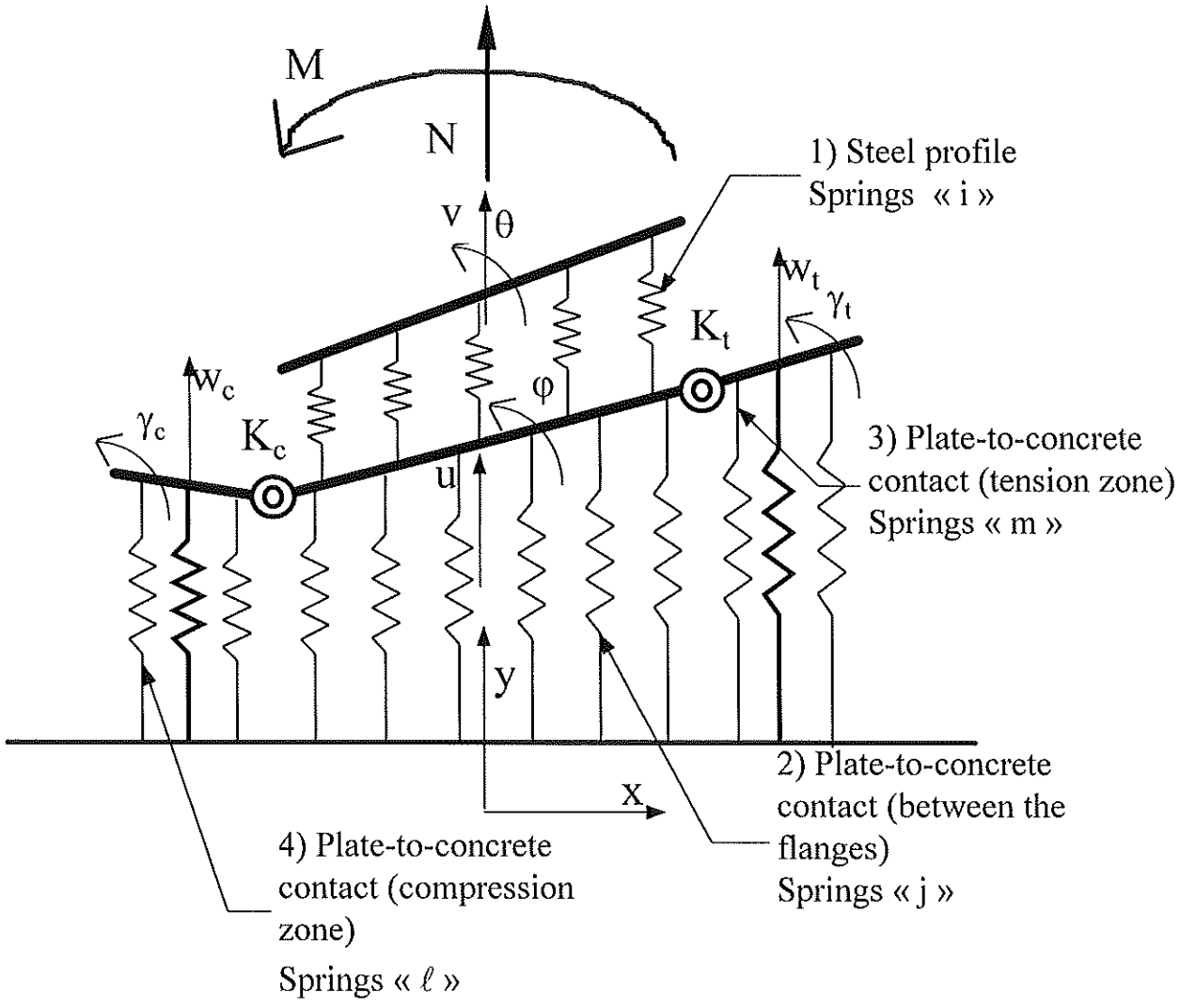

Figure 4.11 - Schematic representation of the mechanical model

The origin of the abscissas (x) is placed on the column axis; the displacement field of the model may be so expressed as follows (see Figure 4.11):

$$\begin{aligned} u(x) &= u + \varphi.x && \text{zone 1} \\ v(x) &= v + \theta.x && \text{zone 2} \\ w_t(x) &= u + \lim_t.\varphi + (x - \lim_t).\gamma_t && \text{zone 3} \\ w_c(x) &= u + \lim_c.\varphi + (x - \lim_c).\gamma_c && \text{zone 4} \end{aligned} \qquad (4.11)$$

where $\lim_t$ and $\lim_c$ designate the abscissas of the flexural springs in the tensile (K_t) and compressive (K_c) zones respectively. The quantities u, v, θ, ϕ, γ_t and γ_c are defined in Figure 4.11. The numbering of the zones (1 to 4) is also shown in Figure 4.11.

Equation 4.10 shows that the deformed state of the system is fully defined by six parameters: u, v, φ, θ, γ_c, γ_t. The determination of these values under loads M and N loads requires six linearly independent equations. These equations are obtained by expressing the vertical and rotational equilibrium of the different zones of the model. First of all, the equilibrium of zone 1, i.e. the upper part of the model representing the steel profile, is expressed. Equation (4.12) relates to the vertical equilibrium and equation (4.13) represents the rotational equilibrium expressed at (0,0) :

$$N + \sum_i F_i = 0 \qquad (4.12)$$

$$M + \sum_i F_i \,.\, x_i = 0 \qquad (4.13)$$

where F_i designates the axial force in the "zone 1" spring i.

In equations (4.12) and (4.13), the sommation applies to all the springs of the zone 1 which represents the column profile subject to combined bending and compressive or tensile forces. The force in a spring may be calculated from the displacements as follows:

$$F_i = K_i.(v_i - u_i) = K_i.\left[(v - u) + x_i.(\theta - \varphi)\right] \qquad (4.14)$$

K_i corresponds to the stiffness of the sring "i".

By substituting equation (4.14) in (4.12) and (4.13), we obtain:

$$N + \sum_i K_i(v - u) + \sum_i K_i.x_i(\theta - \varphi) = 0 \qquad (4.15)$$

$$M + \sum_i K_i.x_i(v - u) + \sum_i K_i.x_i^2(\theta - \varphi) = 0 \qquad (4.16)$$

The vertical equilibrium of the whole lower part of the model, namely zones 2 to 4 writes :

$$-\sum_{i} F_i + \sum_{j} F_j + \sum_{\ell} F_\ell + \sum_{m} F_m = 0 \tag{4.17}$$

The forces in the springs "j", " ℓ " and "m" (see Figure 4.11) can be expressed as follows:

$$F_j = K_j.u_j = K_j.(u + x_j.\varphi) \tag{4.18}$$

$$F_m = K_m.w_t = K_m.\left[u + \lim_t.\varphi + (x_m - \lim_t).\gamma_t\right] \tag{4.19}$$

$$F_\ell = K_\ell.w_c = K_\ell.\left[u + \lim_c.\varphi + (x_\ell - \lim_c).\gamma_c\right] \tag{4.20}$$

By combining equations (4.18) to (4.20) and (4.14) with equation (4.17), the third equation of equilibrium is obtained:

$$\begin{aligned}&\left[\sum_{i} K_i + \sum_{j} K_j + \sum_{\ell} K_\ell + \sum_{m} K_m\right].u - \sum_{i} K_i.v + \\ &\left[\sum_{i} K_i.x_i + \sum_{j} K_j.x_j + \lim_c.\sum_{\ell} K_\ell + \lim_t.\sum_{m} K_m\right].\varphi - \sum_{i} K_i.x_i.\theta \\ &+\left[\sum_{\ell} K_\ell.x_\ell - \lim_c.\sum_{\ell} K_\ell\right].\gamma_c + \left[\sum_{m} K_m.x_m - \lim_t.\sum_{m} K_m\right].\gamma_t = 0\end{aligned} \tag{4.21}$$

The three last equations needed to solve the system are obtained by expressing the individual rotational equilibrium of each of the zones 2, 3 and 4. The moments acting in the end-plate rotational springs can be expressed as follows:

$$M_c = K_c.(\varphi - \gamma_c) \geq 0 \tag{4.22}$$

$$M_t = K_t.(\gamma_t - \varphi) \geq 0 \tag{4.23}$$

As previously explained the stiffnesses K_c and K_t depend on the direction of the bending moment applied to the expended parts of the plate (Figure 4.9). The rotational equilibrium of the interior part of the plate writes :

$$\left[\sum_i K_i.x_i + \sum_j K_j.x_j + lim_c.\sum_\ell K_\ell + lim_t.\sum_m K_m\right].u - \sum_i K_i x_i.v +$$
$$\left[\sum_i K_i.x_i^2 + \sum_j K_j.x_j^2 - K_t - K_c + lim_c^2.\sum_\ell K_\ell + lim_t^2.\sum_m K_m\right].\varphi - \sum_i K_i.x_i^2.\theta \quad (4.24)$$
$$+\left[lim_c.\sum_\ell K_\ell.(x_\ell - lim_c) + K_c\right].\gamma_c + \left[lim_t.\sum_m K_m.(x_m - lim_t) + K_t\right].\gamma_t = 0$$

Equations (4.25) and (4.26) express the rotational equilibrium of the extended parts under tension and compression loads.

$$\left[\sum_\ell K_\ell.(x_\ell - lim_c)\right].u + \left[\sum_\ell K_\ell(x_\ell - lim_c).lim_c + K_c\right].\varphi$$
$$+\left[\sum_\ell K_\ell.(x_\ell - lim_c)^2 - K_c\right].\gamma_c = 0 \quad (4.25)$$

$$\left[\sum_m K_m.(x_m - lim_t)\right].u + \left[\sum_m K_m(x_m - lim_t).lim_t - K_t\right].\varphi$$
$$+\left[\sum_m K_m.(x_m - lim_t)^2 + K_t\right].\gamma_t = 0 \quad (4.26)$$

At this stage the six linearly independent equilibrium equations are available. These can be expressed in the form of a matrix. It is here quite important to note that the stiffnesses K of each spring are tangential ones and are deduced from the component non-linear curves; they vary then with the level of loading applied to the column base. As a consequence, the moment-rotation curve of the column base has to be built step by step by applying successively load increments to the mechanical model and by evaluating the corresponding deformations. This requires, at each loading step, to solve the system of non-linear equations expressed in an incremental format. As the position of all the springs is fixed, the incremental expression of the equilibrium equation is simply achieved (see equation 4.27) by replacing, in the six equations, the displacements u, v, φ, θ, γ_c, γ_t and the external forces applied M and N by their increments.

The springs simulating the anchor bolts belong either to zone 2 in the case of column bases with two anchor bolts- index "j" - or to zones 3 and 4 in the case of column bases with four anchor bolts - indices "m" and " ℓ " -.

$$
\begin{bmatrix}
\sum K_i & \sum K_i.x_i & -\sum K_i & -\sum K_i.x_i & 0 & 0 \\
 & \sum K_i.x_i^2 & -\sum K_i.x_i & -\sum K_i.x_i^2 & 0 & 0 \\
 & & \sum K_i + \sum K_j + \sum K_m + \sum K_r & \sum K_i.x_i + \sum K_j.x_j + \lim_t \sum K_m + \lim_c \sum K_r & \sum K_r.x_r - \lim_c \sum K_r & \sum K_m.x_m - \lim_t \sum K_m \\
 & & & \sum K_i.x_i^2 + \sum K_j.x_j^2 - K_t - K_c + \lim_t^2 \sum K_m + \lim_c^2 \sum K_r & \lim_c \sum K_r.x_r - \lim_c^2 \sum K_r + K_c & \lim_t \sum K_m.x_m - \lim_t^2 \sum K_m + K_t \\
 & & & & \sum K_r.(x_r - \lim_c)^2 - K_c & 0 \\
\text{sym.} & & & & & \sum K_m.(x_m - \lim_t)^2 - K_t
\end{bmatrix}
\begin{Bmatrix} \Delta v \\ \Delta\theta \\ \Delta u \\ \Delta\varphi \\ \Delta\gamma_c \\ \Delta\gamma_t \end{Bmatrix}
=
\begin{Bmatrix} -\Delta N \\ -\Delta M \\ 0 \\ 0 \\ 0 \\ 0 \end{Bmatrix}
\tag{4.27}
$$

The different steps of the iterative procedure which leads to build progressively the deformability curve of the column base are detailed hereunder.

- Let us consider the system in equilibrium under applied forces M_i and N_i. The displacements u_i, v_i, φ_i, θ_i, γ_{ci}, γ_{ti} are associated to these forces. At the beginning of the process, all these quantities are equal to zero.

- As the deformation of the system is known, it is possible to calculate the individual deformation of each spring. From this deformation, the tangential stiffness of the springs may be derived from their F-δ law (Formulae 4.3, 4.7 and 4.8).

- At the beginning of the iterative process, no information is avaible on the behaviour of the system; it is therefore assumed a priori that all the springs are activated and that their stiffness is taken equal to the elastic one.

- Load increments ΔN_{i+1}, ΔM_{i+1}, are applied to the system. On the basis of the tangential stiffnesses calculated above, equation 4.27 is solved to obtain the six increments of displacement Δu_{i+1}, Δv_{i+1}, $\Delta\varphi_{i+1}$, $\Delta\theta_{i+1}$, $\Delta\gamma_{ti+1}$, $\Delta\gamma_{ci+1}$ which are then added to the values already calculated.

- For this new deformed state, the forces acting in the different springs are evaluated. Because of the linearization of the equilibrium equations, the resultant of these forces does not counterbalance perfectly the moment and axial load applied. The difference between these two quantities is termed "out-of-equilibrium forces".

- To compensate for this lack of accuracy, equation (4.27) is solved again by replacing ΔN_{i+1} and ΔM_{i+1} respectively by the values of the out-of-equilibrium axial force and the out-of-equilibrium

moment. New increments of displacement are obtained which are again added to the previous values, and this iterative procedure is applied until the out-of-equilibrium forces are small enough to be ignored. At this moment, the deformed state of the system under the $N_i+\Delta N_{i+1}$ and $M_i+\Delta M_{i+1}$ loads is finally known.

- A new increment of forces is then applied, and the iterative process described here-above is reactivated until failure is reached, i.e. when:

  - the system of equations have singularities, what only occurs when the resistance of all the springs of zone 1 or all the springs of zones 2 to 4 is exhausted;
  - the system of equations diverges or requires too many iterations to converge, thereby signifying that the resistance of a large number of springs is exhausted and that the equilibrium is practically impossible to satisfy;
  - the displacements observed become too large, thus falling outside the scope of the model (excess of deformation capacity in some components).

In the next section, comparisons between the mechanical model and the experimental results described in chapter 2 are presented.

In these applications, the failure of the column base is reached for the first above-described two reasons; the concrete crushes or the anchor bolts breaks in tension (in most of the tests) or the steel profile yields (test PC4.30.1000).

4.4 Comparison with the experiments.

Figure 4.12 to Figure 4.23 present comparisons between the mechanical model described in the foregoing paragraphs and the twelve experimental tests results.
The curves presented in these figures are the moment-rotation curves of the column bases. With regard to the mechanical model, the graph shows the variation of M as a function of θ, i.e. the rotation measured at the base of the steel profile, with due account being taken of the yielding phenomena occurring in the latter.
For the configurations with two anchor bolts the theoretical curves obtained using the PENSERINI method [5] have also been plotted. It is clear that the agreement between the latter and the experimental tests is far from convincing (Figure 4.12 to Figure 4.17). This is simply because the tests carried out in Liège are largely outside the scope of the PENSERINI model.

Examination of Figure 4.12 to Figure 4.14 presenting tests PC.15 (two bolts - 15 mm plate) reveals an excellent agreement between the mechanical model and experimentation. The initial stiffness of the moment-rotation curve is accurately predicted by the model; the progressive yielding of the column base is perfectly predicted by the theory. On the other hand, the agreement is less satisfactory for the ultimate load; its remains however quite acceptable (scatter of 5 to 10% maximum). This is due to the great complexity of behaviour when the different components of the column base are close to collapse:

- concrete is a material whose mechanical properties can vary considerably according to the quality of the compaction. Furthermore, the crushing of the concrete under local forces is not an easy phenomenon to model;
- the anchorage of the bolts in the concrete is aleatory. In fact, contrary to what was expected, the anchorage of the bolts by the concrete was not sufficient enough to prevent a relative overall movement between the bolt and its support. Fortunately, these movements only occurred in the case of very high tension forces at the end of the test, and thus only altered the ultimate load.
- the displacements at the end of the test become quite significant, what leads to geometry changes which are not correctly taken into account in the mechanical model.

Despite this, and considering the curves as a whole, the general agreement between the mechanical model and the tests can be regarded as being quite good.

A similar conclusion could be drawn at Figure 4.15 to Figure 4.17 relating to tests PC2.30, except for test PC2.30.100 (Figure 4.15).

Some investigations have shown, however, that the only way to come to a better agreement for tests PC2.30.100, with the model, was to reduce the stiffness of the concrete without modifying its ultimate strength.
In other words, the lack of stiffness in the concrete block appears as the main reason to explain the rather poor agreement obtained in this case. And, in fact, that is what happened in test PC2.15.100 as explained in section 2.4.2.

Figure 4.18 and Figure 4.20 relate to PC4.15 tests. Again, the agreement is seen quite acceptable.

Finally, Figure 4.21 to Figure 4.23 show a moderate agreement between theory and experimentation. While test PC4.30.400 (Figure 4.22) gives excellent results, test PC4.30.100 seems to suffer from the same problem than test PC2.30.100, i.e. an actual stiffness for the concrete lower than the theoretical prediction. Finally, test PC4.30.1000 seems to be well described by the mechanical model (Figure 4.23) when the moment is lower than half its ultimate value. But, as already said, a progressive buckling of the column flange in compression has been observed during the test and it has been previously pointed out that this failure mode is not included in the model. This probably explains the additional deformability reported during the test.

In conclusion, the agreement between the mechanical model and the experimentation can be considered as quite satisfactory, even good. Few discrepancies have been observed. These, however, can be explained and they do not put the general validity of the proposed rules in question again. It must not be forgotten that these rules have been rigorously derived, i.e. without a single empirical parameter, and are identical for the twelve tests being considered.

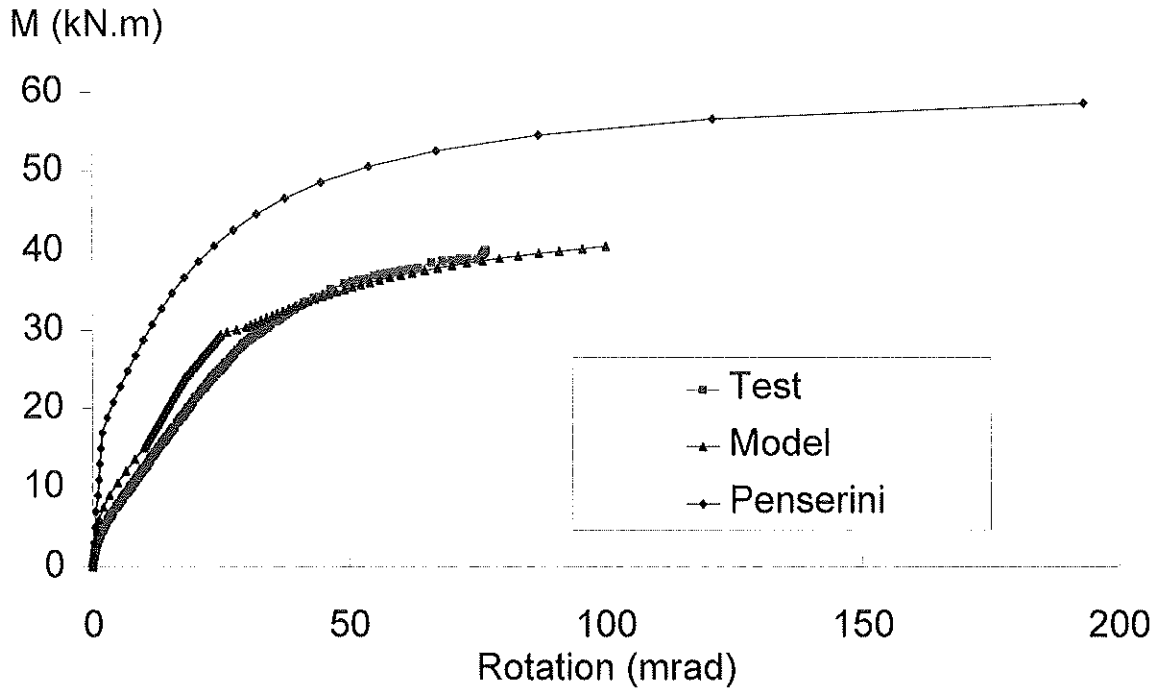

Figure 4.12 - Comparison between the tests and the mechanical model. Test PC2.15.100

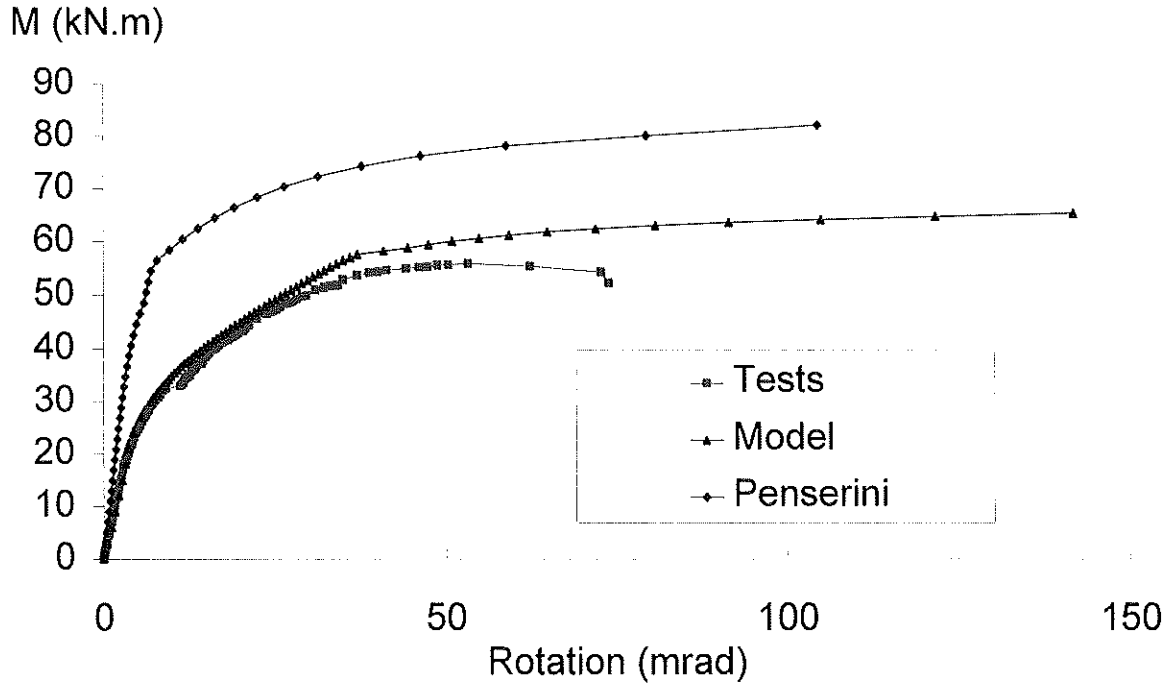

Figure 4.13 - Comparison between the tests and the mechanical model. Test PC2.15.600

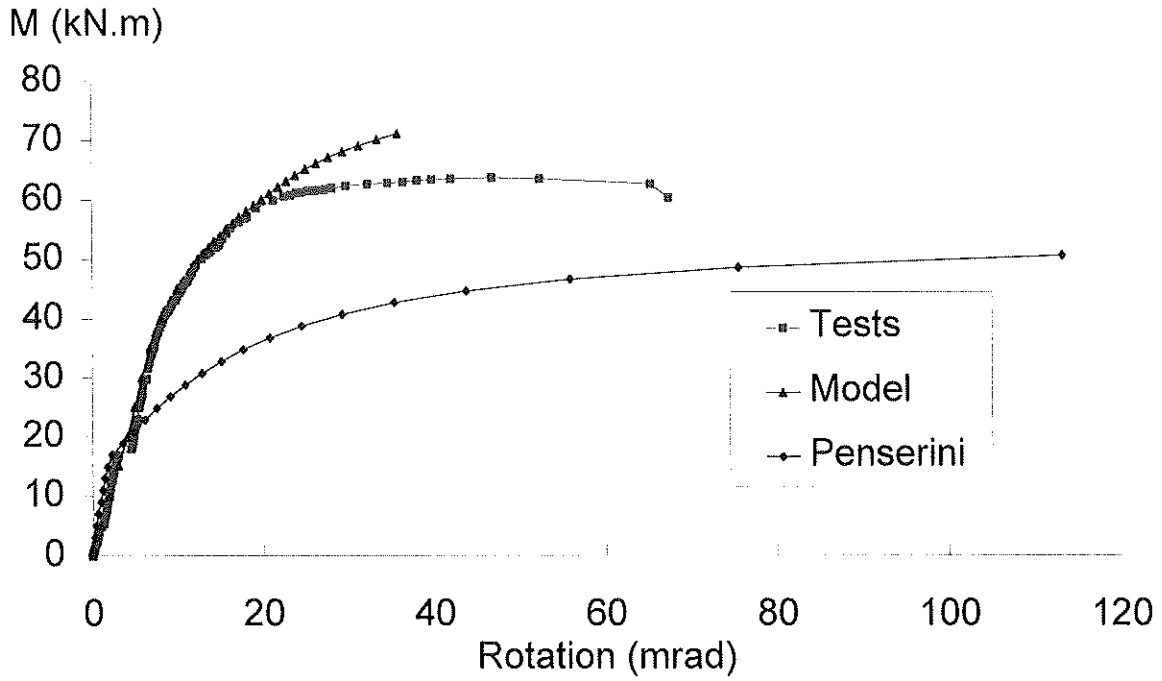

Figure 4.14 - Comparison between the tests and the mechanical model. Test PC2.15.1000

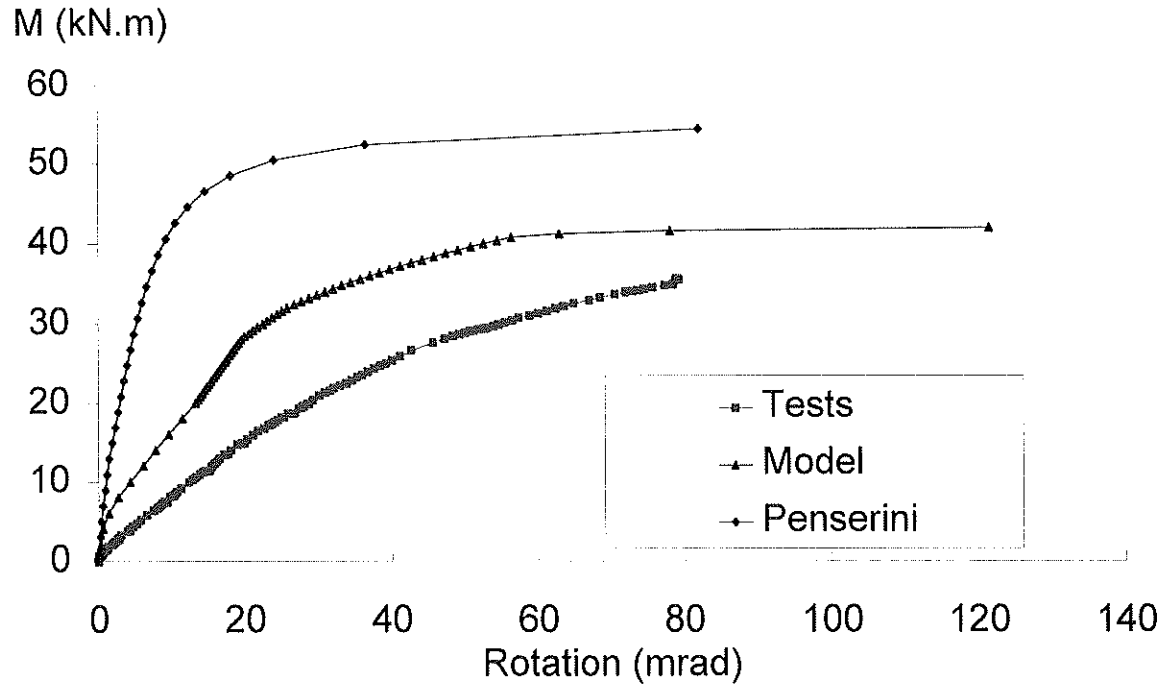

Figure 4.15 - Comparison between the tests and the mechanical model. Test PC2.30.100.

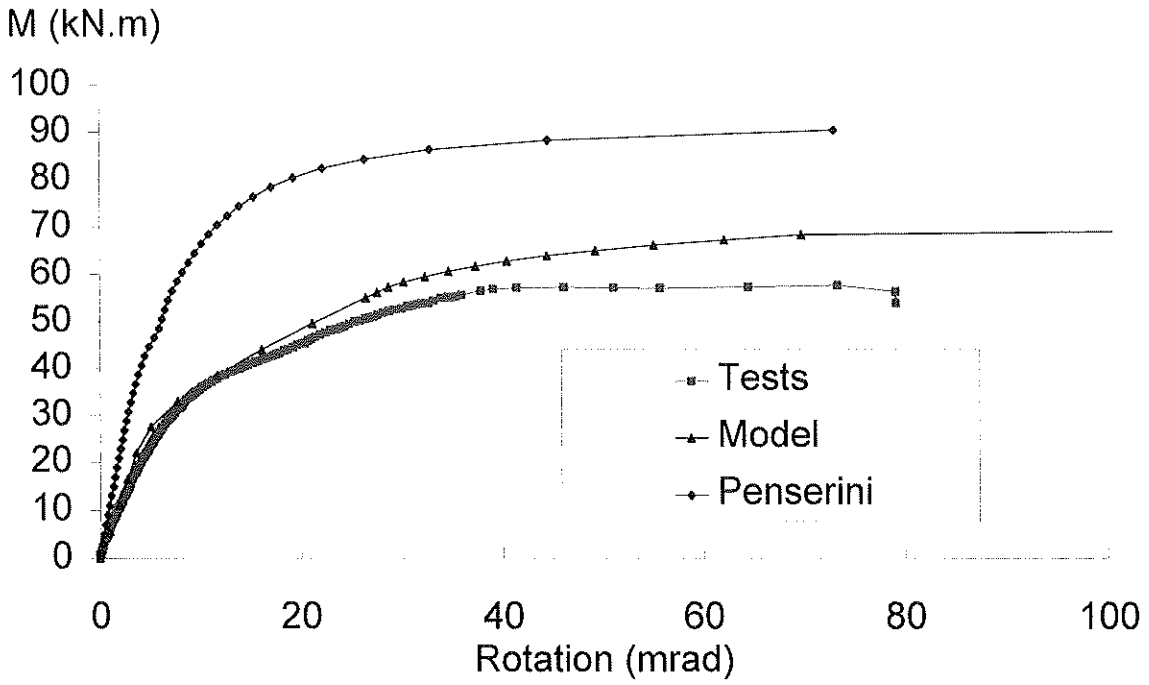

Figure 4.16 - Comparison between the tests and the mechanical model. Test PC2.30.600

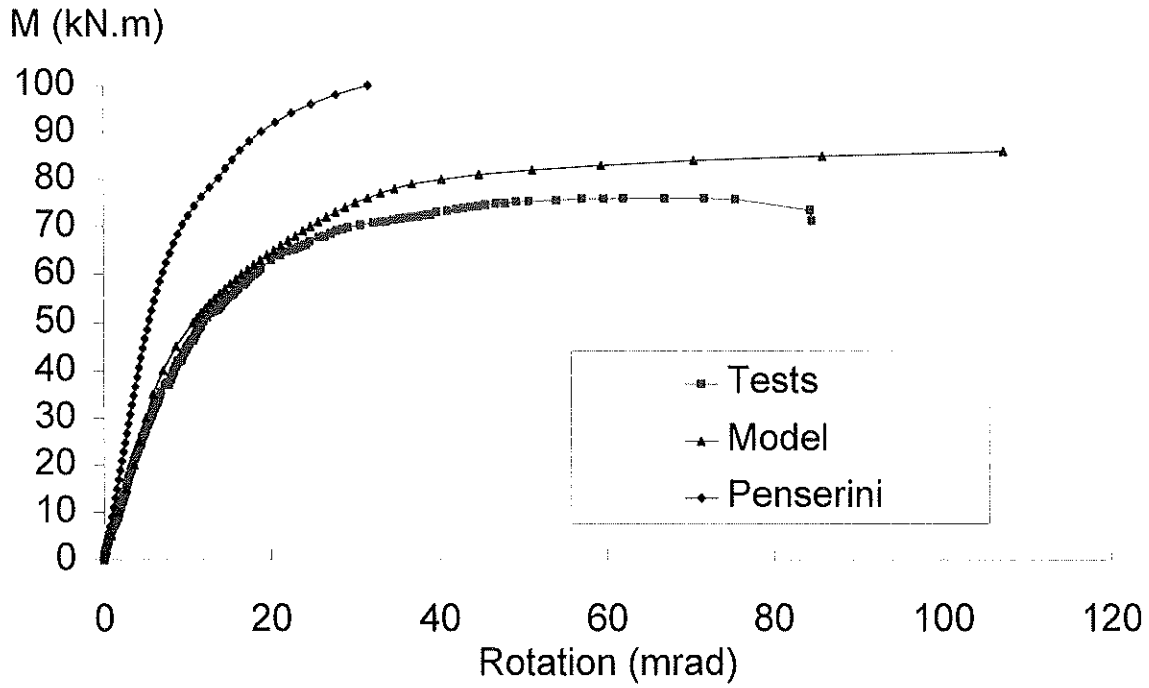

Figure 4.17 - Comparison between the tests and the mechanical model. Test PC2.30.1000.

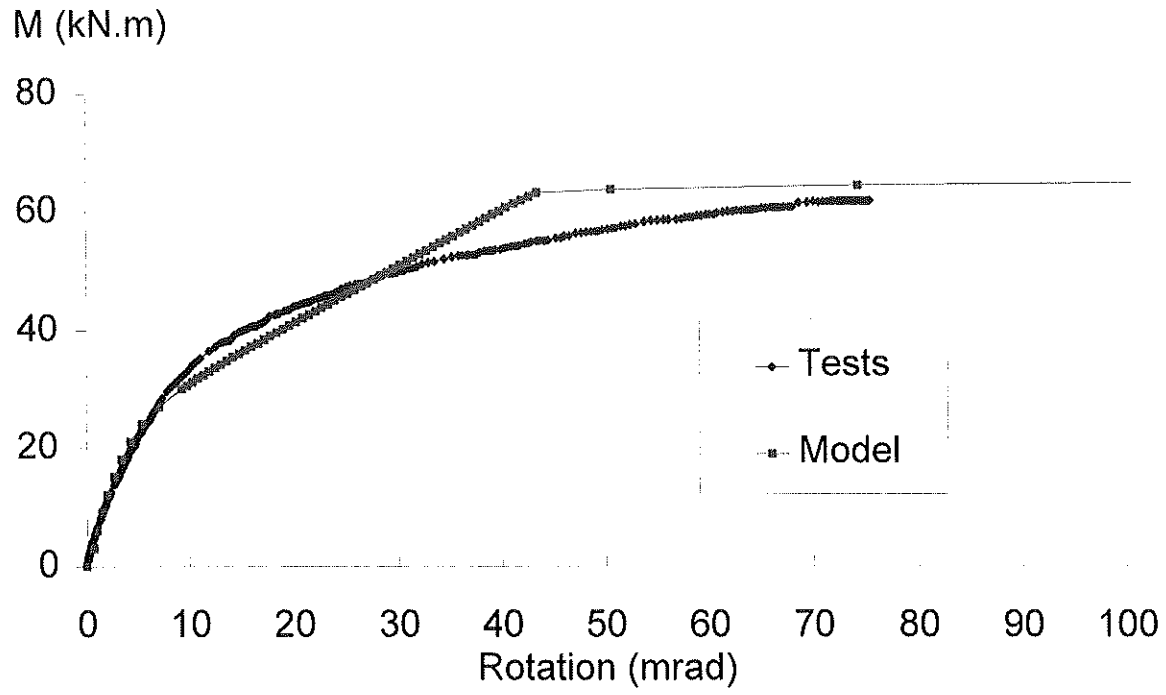

Figure 4.18 - Comparison between the tests and the mechanical model. Test PC4.15.100.

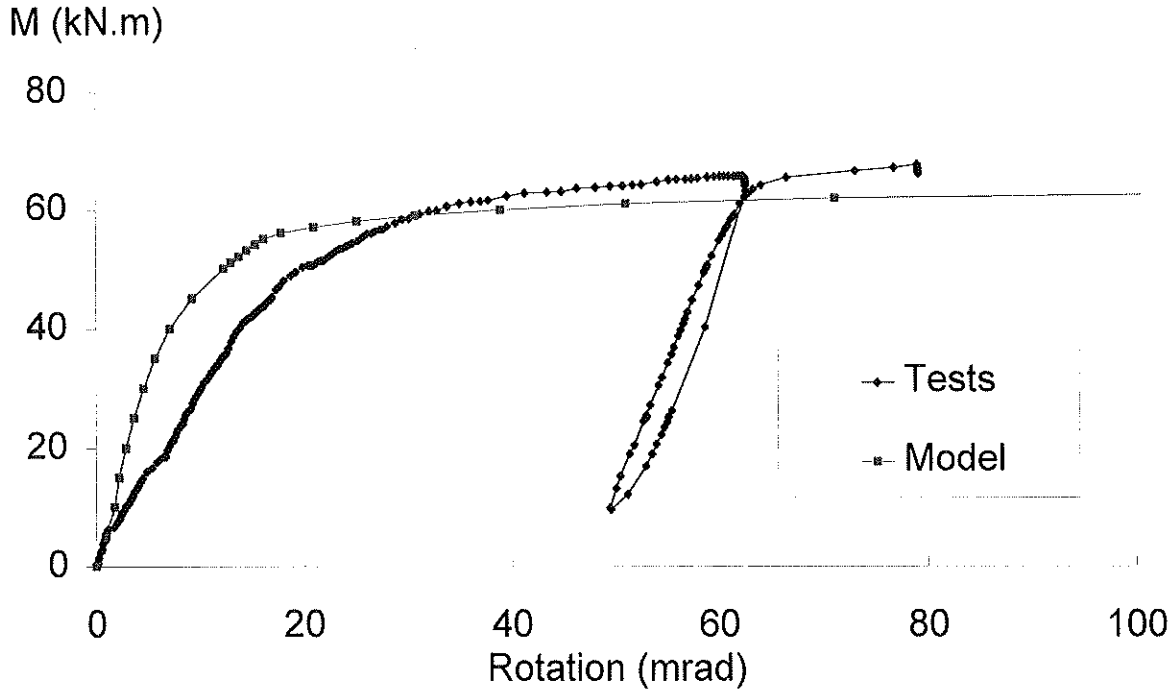

Figure 4.19 - Comparison between the tests and the mechanical model. Test PC4.15.400.

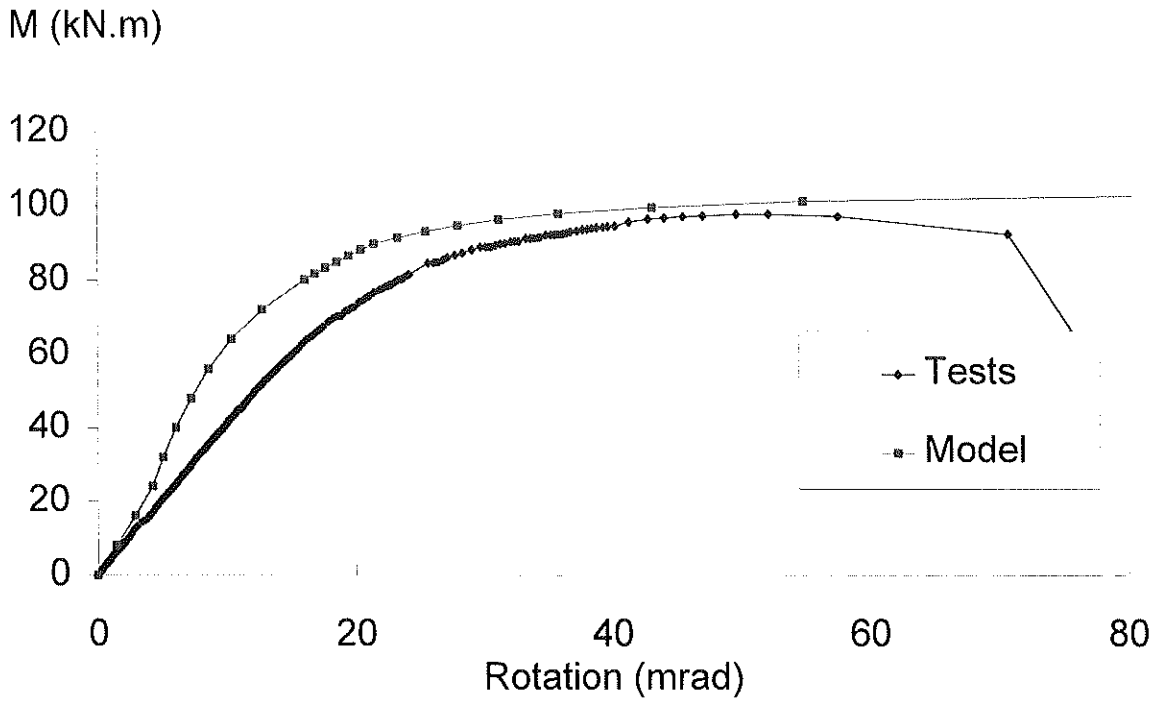

Figure 4.20 - Comparison between the tests and the mechanical model. Test PC4.15.1000.

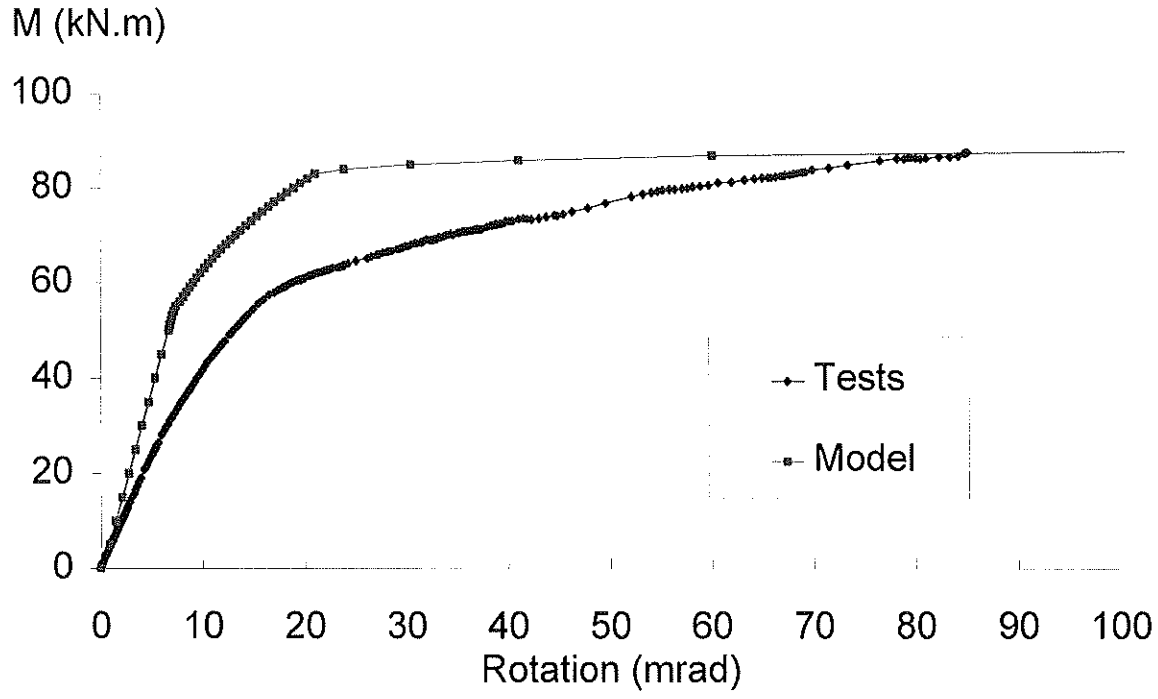

Figure 4.21 - Comparison between the tests and the mechanical model. Test PC4.30.100

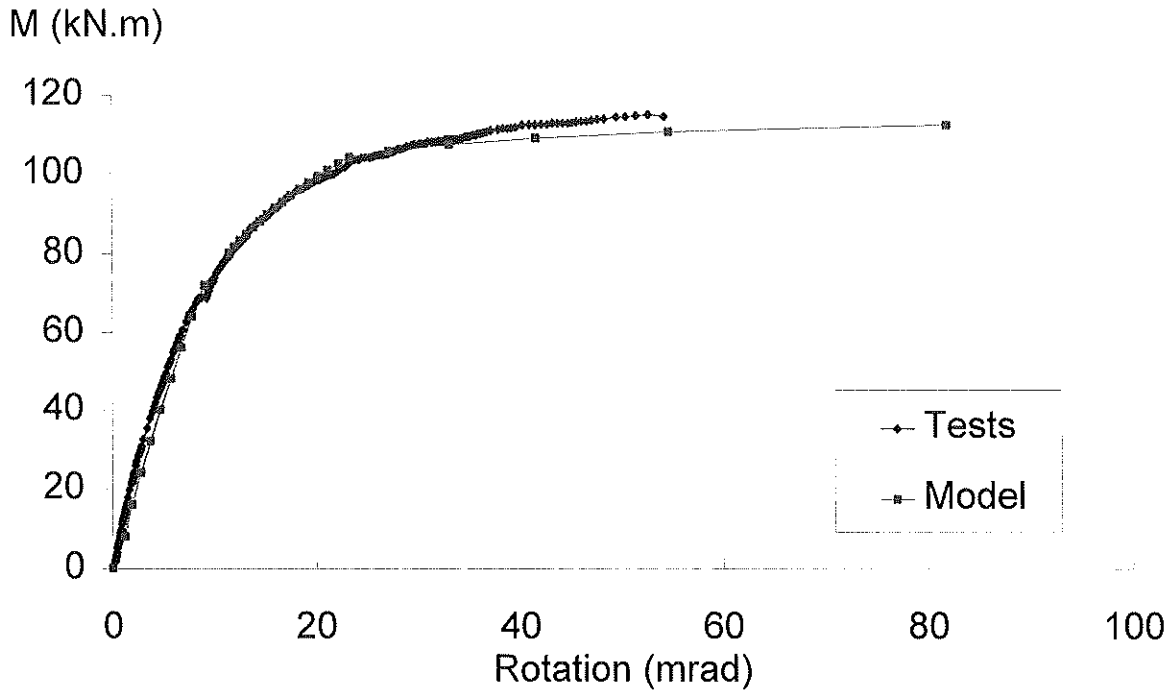

Figure 4.22 - Comparison between the tests and the mechanical model. Test PC4.30.400.

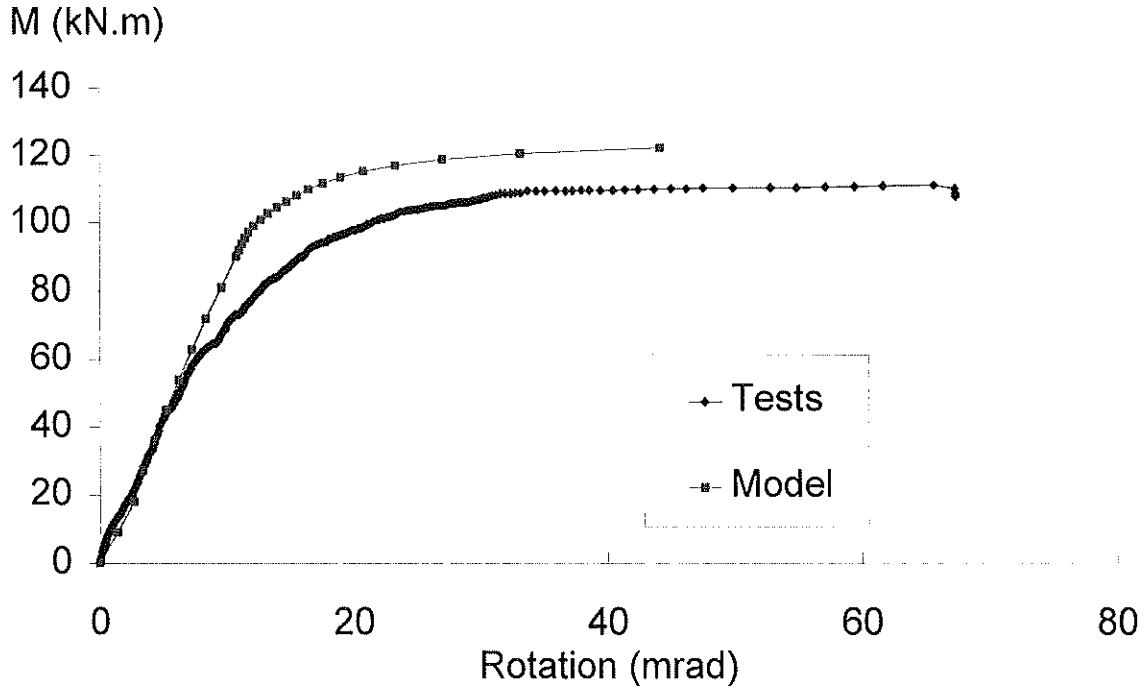

Figure 4.23 - Comparison between the tests and the mechanical model. Test PC4.30.1000.

5. CONCLUSIONS AND FURTHER DEVELOPMENTS

Twelve column bases constituted of welded plates connected to the concrete foundation by means of two or four anchor bolts have been tested in Liège in the frame of the COST C1 European Project. The results of these ones are presented in the report and the main influence of the selected parameters (number of anchor bolts, thickness of the base plates and ratio between bending moment and axial compressive force) is extensively discussed.

On the basis of the knowledge got from these tests and from the available literature, a simple analytical model aimed at predicting the ultimate and design resistances has been developed and validated through comparisons with the experiments.
The model appears as an application of the principles of the component method, with references to annexes L and J of Eurocode 3 for what regards the characterization of the individual basic components.

A complete model requires also nowadays the prediction of the stiffness properties in rotation of the column bases.

However, the complexity of the problem is such that the development of a simple and reliable stiffness model appears still now as quite contingent. It has therefore been decided to focus in this report on the development of a scientific tool, i.e. a mechanical model, allowing, through rather long and iterative calculation procedures, to simulate accurately the non-linear response of the column bases from the first loading steps to failure.

Such a tool, the validity of which is demonstrated through comparisons with experiments, allows to deeply understand the behaviour of the column bases and of their constitutive components, the inherent interactions and the way failure occurs.

Through the use of this tool in parametric studies, the development of a reliable stiffness model may be contemplated in the future, and more especially in the frame of the present CRIF two-years projects on column bases where complementary experiments on column bases with two anchor bolts subjected to uniaxial major or minor axis bending have been recently performed.

ACKNOWLEDGMENTS

The authors of the present report would like to thank warmly the staff of the M.S.M. laboratory for their good work in the execution of the tests, an those who contributed to the realisation of this document, especially Jacqueline Habotte for the secretariat work, and Victor Marinus and Ashok Lalloo.

REFERENCES

[1] Eurocode 3.
Design of Steel Structures. Part 1.1. : General Rules and Rules for Buildings,
European Prestandard - ENV 1993-1-1, February 1992.

[2] Eurocode 3, Annex L on "Design of Column Bases".
European Prestandard - ENV 1993-1-1, February 1992.

.

[3] Eurocode 3, Revised Annex J on "Joints in Building Frames".
CEN/TC 250/SC3-N 419 E, Brussels, June 1994.

[4] WALD F.
Patky sloupu - Column Bases - CVUT - Czech Technical University, Prague 6, 1995.

[5] PENSERINI P.
Caractérisation et modélisation du comportement des liaisons structure métallique-fondation, Ph. D. Thesis, University Pierre et Marie Curie, Paris 6, 1991.

[6] JASPART J.P.
Etude de la semi-rigidité des noeuds poutre-colonne et son influence sur la résistance et la stabilité des ossatures en acier.
Ph. D. Thesis, Department M.S.M., University of Liège, 1991.

FURTHER READING

- HON K.K., MELCHERS R.E.
  Moment-Rotation Curves for "Pinned" Column-Bases. The Structural Engineer, vol. 65B, n° 3, pp. 54-59, 1987.

- BIJLAARD F.S.K.
  Rekenregels voor het ontwerpen van kolomvoet-platen en expérimentale verificatie.
  Report n° BI-81-51/63.4.3410, IBBC-TNO, Delft, 1982.

- DEWOLF J.T., SARISLEY E.F.
  Column Base Plates with Axial Loads and Moments. Journal of the Structural Division, ASCE, vol. 106, n° ST11, pp. 2167-2185, 1980.

- PICARD A., BEAULIEU D.
  Behaviour of a Simple Column Base Connection, Canadian Journal of Civil Engineering, vol. 12, n° 1, pp. 126-136, 1985.

- SEIFERT J., WALD F., SVOBODA P.
  Column-Base Stiffness Tests, Czech Technical University Research Report, Prague, 1991.

- THAMBIRATNAM D.P., PARAMASIVAM P.
  Base Plates under Axial Loads and Moments, Journal of Structural Engineering, vol. 112, n° 5, pp. 1166-1181, 1986.

- TRAUNER L., SKRABL S., ZLENDER B.
  Spread Hinge-tied Foundation.
  University of Maribor, Faculty of Technical Sciences, Slovenia, 1993.

- JIANGUO X., WEIJAN G., ZHENPENG G., ZHAOHUI D.
  Overturning Resistance and Rotation of Foundation in Soil under Lateral Loading, Computers and Geotechnics, n° 8, pp. 157-174, 1989.

- LESCOUARC'H Y.
  Les pieds de poteaux articulés en acier. C.T.I.C.M., April 1982.

- MELCHERS R.E.
  Column-Base Response Under Applied Moment. Journal of Constructional Steel Research, n° 23, pp. 127-143, 1992.

- NAKASHIMA, S., IGARASHI S., KADOYA H., SUZUKI T.
  Experimental Behaviour of Encased Steel Column-Base Connections, IABSE Symposium Mixed Structures, part A, Brussels, pp. 289-295, 1990.

- NAKASHIMA S., IGARASHI S., SUZUKI T.
  Behaviour of Full Scale Exposed Type Steel Square Tubular Column Bases under Lateral Loading, IABSE Symposium, part A, Helsinki, pp. 148-152, 1989.

- WALD F.
  Column-Base Connections, A Comprehensive State-of-the-Art Review, Prague, February 1993.

- WALD F., ZDENEK S., PERTOLD J.
  Column-Base Connections, Strength Design, Prague, February 1994.

- WALD F., SIMEK I., BEZDEK P.
  Data-Bank of Column Base Connections, COBADAT Alfa, CTU, Prague, 1993.

ANNEX

EXPERIMENTAL AND PREDICTED MOMENT RESISTANCES FOR JOINTS

EXPERIMENTAL AND PREDICTED MOMENT RESISTANCES FOR JOINTS

1. INTRODUCTION

The resistance of any structural element appears traditionally as the most important mechanical property to consider in the design process. Its precise evaluation through appropriate tools (analytical formulae, laboratory tests, finite element simulations, ...) is a prerequisite to an economical and safe structural design.

This statement is agreed by all, but the definition to give to the term « resistance » seems to differ substantically from one person, one institution or one country to another. This situation is quite embarrassing for different reasons :

- The tools proposed in the literature for the evaluation of the resistance have to be first validated through comparisons with test results and the compared values should obviously refer to the same definitions.
- When the evaluation tools for resistance are codified or recommended in design handbooks, their use should be made in a appropriate way.
- The level of resistance to be considered in the design process depends on the type of frame analysis which is performed, and any unconsistency should be avoided.

The terms used to define the resistance are quite important. Expressions like : « design resistance », « actual resistance », « ultimate resistance », « plastic resistance », ... seem not to be understood in a similar way over the world.

In this particular context, it appears quite necessary, through the present annex, to clarify the different terms listed here above and to define them in a proper way so to avoid confusions and misunderstandings.

All the definitions are illustrated in the particular case of structural joints; they however apply to any structural element and can therefore be easily generalized.

2. DEFINITIONS

A clear distinction has to be made first between resistances obtained through laboratory tests and through the application of analytical or numerical models.

2.1 Resistances from tests

In laboratory tests, moment-rotation curves are traditionally reported. Their shape differs from one specimen tested to another, but three main rotational responses may be identified :

- M-ϕ curves with quite infinite ductility (figure 1.a);
- M-ϕ curves with good but finite ductility (figure 1.b);
- M-ϕ curves with quite limited ductility (figure 1.c).

The maximum resistance than the joint is able to transfer is said ***ultimate*** and named $M_{Ru,test}$.

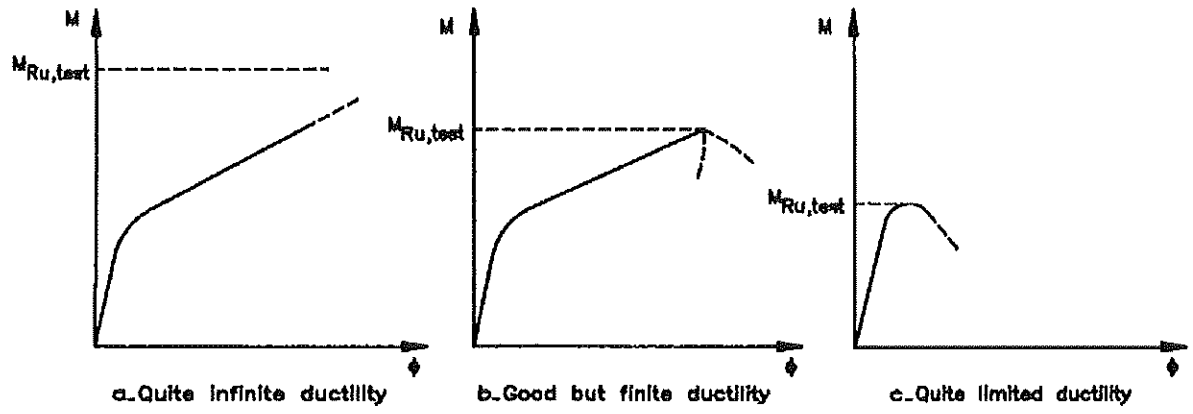

Figure a.1 : Ultimate resistances from tests

For the first category (figure 1.a), the ductile behaviour is such that the ultimate moment resistance of the joint can not be reached during the test, often because of too high displacements in one of the connected members. The ultimate resistance can therefore not to be reported and remains unknown.

For the second and third categories (figure 1.b and 1.c), the ultimate resistance is reached because of the brittle failure - bolts for instance - or the local instability - column web in compression, beam flange and web in compression - of one of the constitutive components of the joint. The value of the ultimate resistance is so clearly identified.

The ductile response of the joint is the result of the progressive yielding of one or more of the components. The stresses extend far beyond the yield stress of the materiel, so developing strain-hardening. This provides to the moment-rotation curves a bi-linear response as shown in figure 1.a. In some cases, this progressive yielding is interrupted by the brittle failure or the instability of a

component, what limits the ductility and the bi-linear character of the curves, as illustrated in figure 1.b and 1.c.

Figure 2 points out the influence of the strain hardening on the moment-rotation curves. For a perfectly elastic material, the moment-rotation would peak at a resistance level named $M_{Rp,test}$, which can be roughly defined as the plastic resistance of the joint. The word « plastic » is quite appropriate as long as yielding phenomena develop and the full plastic resistance of the joints is reached, as for beam and column sections. This is the case for category 1 and 2 curves (see figures 3.a and 3.b). In category 3 curves, no strain-hardening occurs and the two $M_{Rp,test}$ and $M_{Ru,test}$ values coincide; the word « plastic » is still justified if the buckling or the instability occurs just after the plastic resistance of the joint is reached. It is no more acceptable for joints where the instability phenomena or brittle failures precedes the full plasticity. This is why it is suggested here to define $M_{Rp,test}$ as the « **pseudo-plastic** » resistance of the joint but keep anyway the subscript « p » for simplicity.

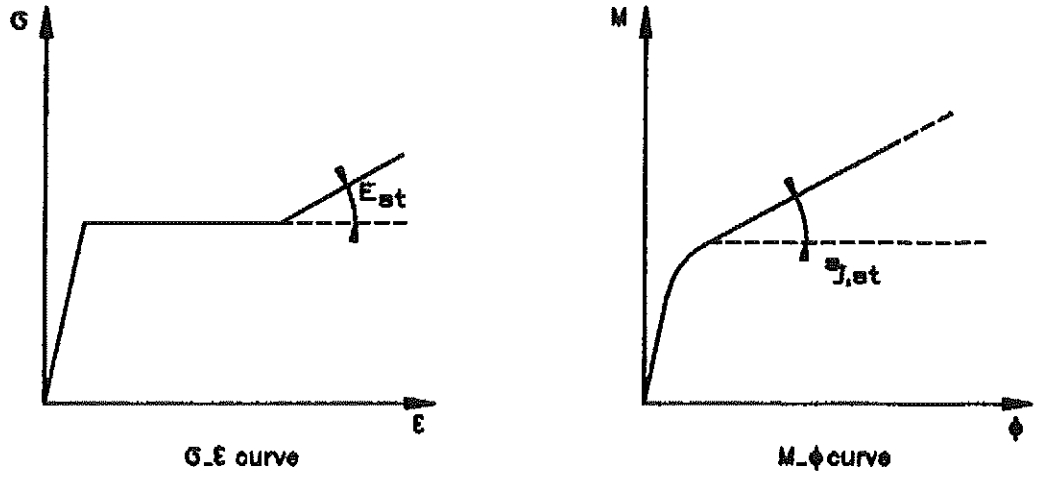

Figure a.2 : Influence of strain-hardening

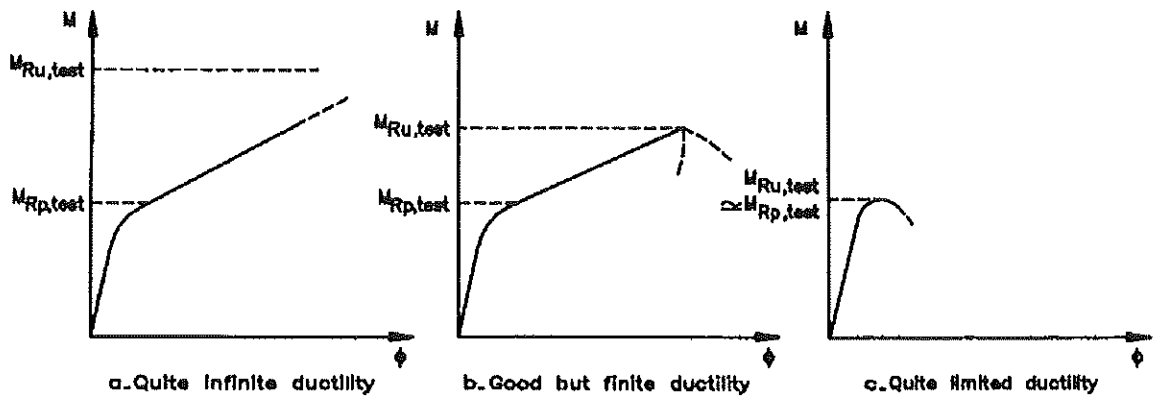

Figure a.3 : Ultimate and pseudo-plastic resistances from tests

Lastly, the maximum **elastic** moment resistance $M_{Re,test}$ of the joint may be usually identified, together with the initial elastic rotational stiffness $S_{j,i}$ (Figure 4).

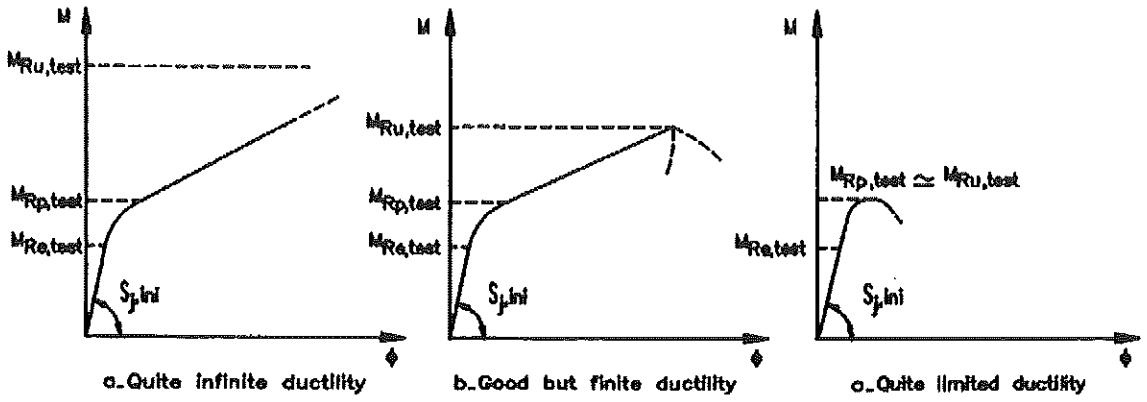

Figure a.4 : Ultimate, pseudo-plastic and elastic resistances from tests

For sake of completion, it has to be mentioned that membranar effects may sometimes develop in constitutive joint components, as a result of their yielding and of the corresponding deformation (as in thin end-plates and flange cleats in bending, for instance). The strain hardening stiffness $S_{j,st}$ is so increased by a this membranar contribution $S_{j,m}$ as pointed out in figure 5. The stiffness characterizing the second branch of the M-ϕ curve located beyond $M_{Rp,test}$ is therefore said « post-limit » ($S_{j,post-limit}$ in figure 5).

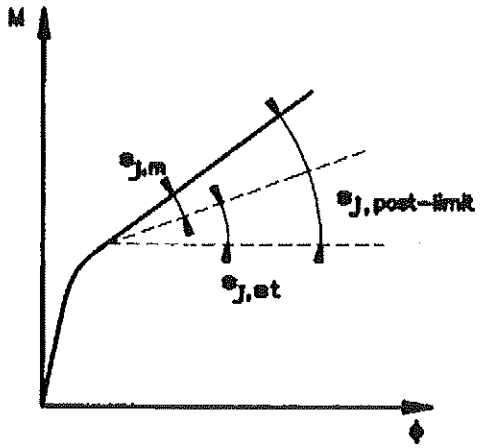

Figure a.5 : Definition of the post-limit stiffness

2.2 Resistances from models

In order to validate prediction tools for resistance, comparisons with tests are usually performed. For sake of consistency, quantities corresponding to similar definition have to be compared. The appropriate moment resistances from the tests and from the models have therefore to be selected, according the level of sophistication of the model.

The more sophisticated models provide the user with a full non linear curve covering the successive loading steps from the first beginning to failure. Before using these models, the **actual** values of the mechanical steel properties for all the joints components are measured; they are used further as data for the models. The **pseudo-plastic** resistances from tests and models can then be directly compared. Similar test-model comparisons can be carried out with **ultimate** resistances, as long as the $M_{Ru,test}$ value can be derived. This requires the measurement of the actual ultimate stress values in order to derive the ultimate yielding resistance. Local instabilities can obviously limit the ultimate joint resistance to a lower value, as for category 2 and 3 curves. The evolution of the rotational stiffness is also often predicted by the sophisticated models. A direct comparison between full non linear curves from test and model can therefore be contemplated (see figure 6).

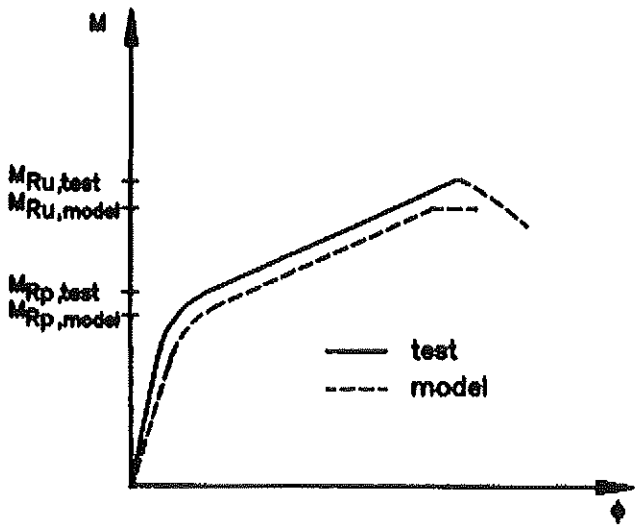

Figure a.6 : Possible comparison between models and tests

Less sophisticated models exist; they allow to derive the **pseudo-plastic** and/or the **ultimate** resistances only. For design purposes, strain-hardening and membranar contributions to the moment resistance are systematically neglected, so limiting the transfer of moment between the connected members to $M_{Rp,model} \approx M_{Rp,test}$. The concept of plastic hinge idealization is so followed, and the length of the yield plateau, which decreases from category 1 to 3, as shown in figure 7, determines the so-called available plastic rotation of the joint.

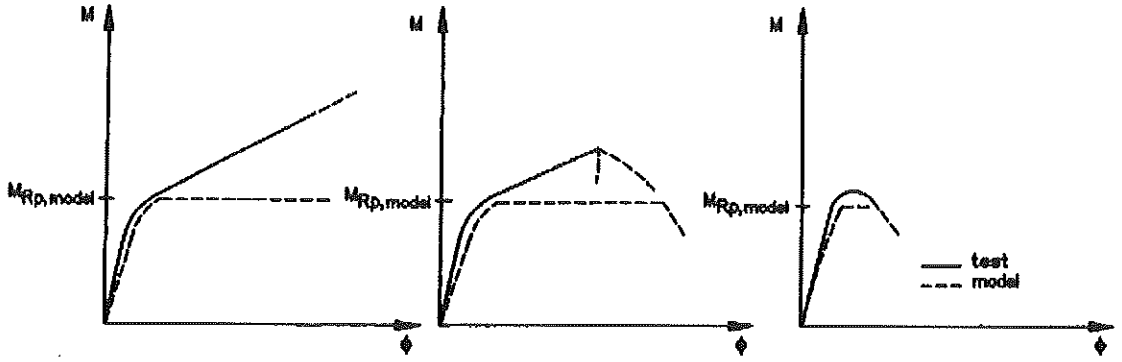

Figure a.7 : Plastic hinge idealization

In an usual design process, the actual values of the yield stresses are unknown and reference has to be made to characteristic values sometimes called « nominal ». The introduction of these characteristic values into prediction models allow to derive **characteristic** moment resistances M_{Rk}.

Furthermore, modern codes, as Eurocodes, follow a semi-probalistic approach for structural safety. The resistance to be used accordingly are design ones and not characteristic ones. They are obtained through the application of the above mentioned models in which design values of the yield stresses are introduced. These ones are derived quite easily by dividing the **characteristic** values of the yield stresses by an appropriate partial safety factor γ. The so defined **design** moment resistance is named M_{Rd}.

In the case of components exhibiting a quite brittle behaviour (bolts in tension, welds, ...), it has to be mentioned that it is referred to f_u and not f_y in the expressions of their pseudo-plastic, characteristic and design resistances, what is not surprising for such « category 3 » components.

3. CONCLUSIONS

Figure 8 illustrates the test and model moment resistances which are defined in the present annex in the particular case of the Eurocode 3 tri-linear model for joints. It indicates that the only comparisons which can be carried out between tests in laboratory and the Eurocodes models are on « **pseudo-plastic** » values ($M_{Rp,test}$ and $M_{Rp,model}$).

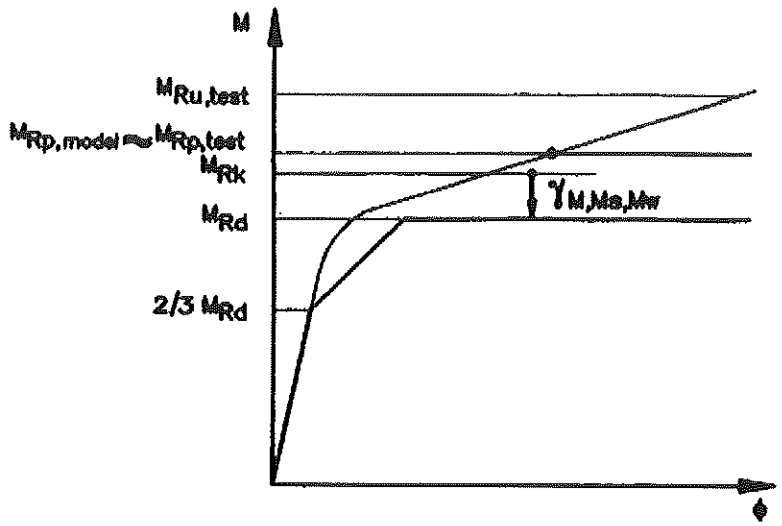

Figure a.8 : Test and model moment resistances (EC3 model)

To derive $M_{Rp,test}$, actual measured values of the yield (or ultimate for brittle components) stresses and partial safety factors γ_{M0} (steel), γ_{Mw} (welds) and γ_{Mc} (concrete) equal to 1,0 , and γ_{Mb} (bolts) equals to 0.9 have to be considered.

From the models giving $M_{Rp,model}$, characteristic and design values can be derived. The better are those of interest for practical design purposes.